

SIMULATION OF ASSISTIVE
GROUSER MECHANISM FOR USE
ON LIGHTWEIGHT WHEELED
ROBOT FOR TRAVERSING ON
UNCONSOLIDATED SOFT SAND
INCLINES

FINAL REPORT
RDU1703191

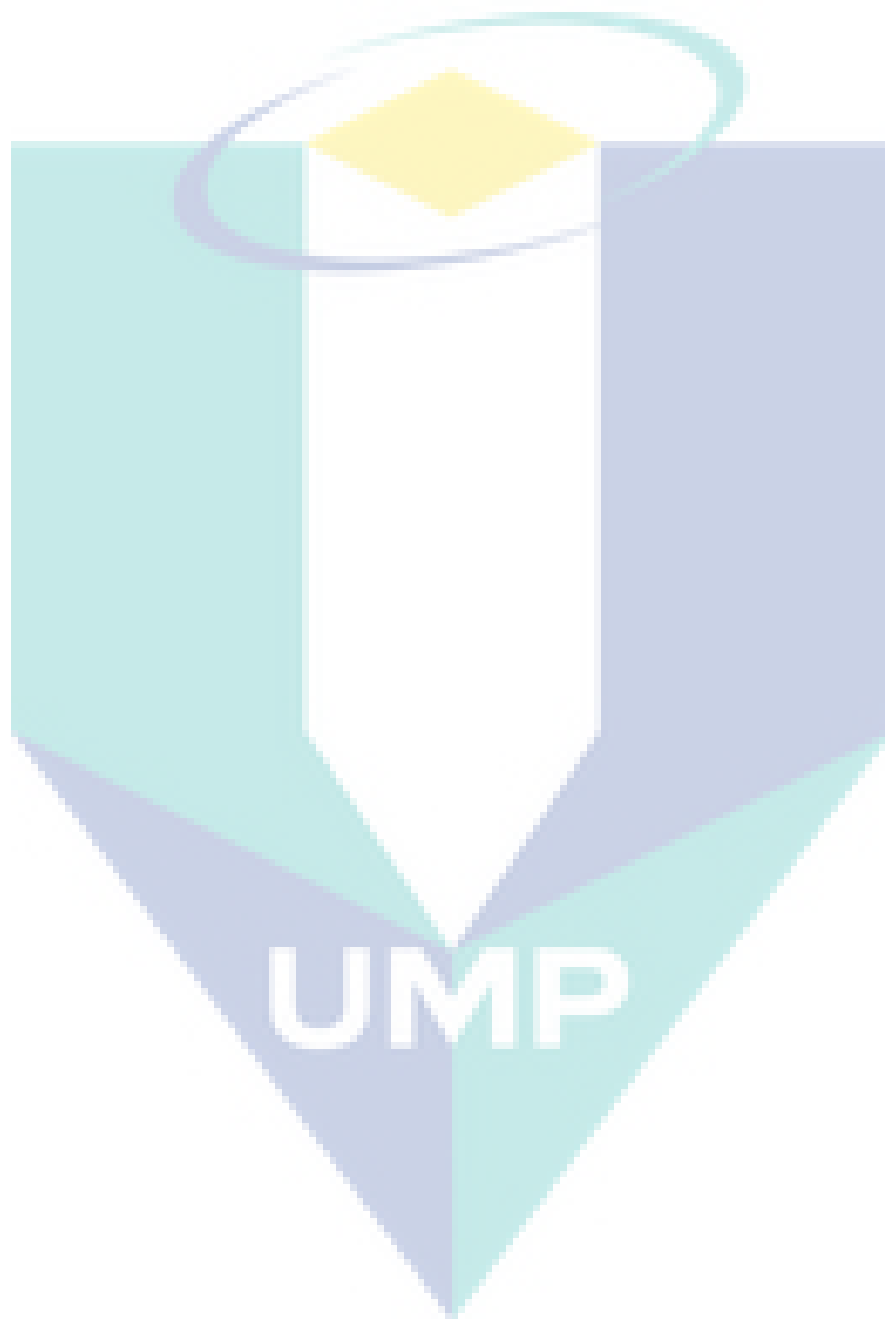
PROJECT LEADER: Dr. AHMAD NAJMUDDIN BIN IBRAHIM

UMP

TABLE OF CONTENT

TABLE OF CONTENT.....	i
CHAPTER 1	1
INTRODUCTION.....	1
1.1 Research Overview	1
1.2 Research Motivation	4
1.3 Problem Statement	6
1.4 Research Objectives	8
1.5 Research Scopes	8
1.6 Research Contribution.....	9
1.7 Thesis Organization/Outline.....	9
CHAPTER 2	10
LITERATURE REVIEW	11
2.1 Introduction	11
2.2 Terramechanics Modelling.....	11
2.3 Computational Fluid Dynamics (CFD)	12
2.4 Finite Element Method (FEM).....	12
2.5 Discrete Element Method (DEM)	13
2.6 Previous Works using Discrete Element Method (DEM)	14
2.7 Referred Case Study.....	16
2.7.1 Wheeled rover mechanism.....	16
2.7.2 Mobility testing set up	18
2.7.3 Result after mobility testing.....	19
2.7.4 Discussion and conclusion for mobility testing	22
2.8 Conclusion.....	23
CHAPTER 3	25
RESEARCH METHODOLOGY	25
3.1 Introduction	25
3.2 Research Methodology Process	25
3.3 Research Component.....	27
3.3.1 Prototype Design	27

3.3.2	Development Model	29
3.3.3	Software Tool.....	30
3.4	DEM Simulation	30
3.5	Simulation Preparation for Conventional Wheel Rover and Modified Wheel Rover	33
3.5.1	Wheel Building	34
3.5.2	DEM Setup	38
3.6	Simulation Preparation for Assistive Grouser Movement Model.....	38
CHAPTER 4		40
RESULT AND DISCUSSION		40
4.1	Introduction	40
4.2	Performance Evaluation for Conventional Rover and Modified Rover	40
4.2.1	Particle Velocity Pattern	40
4.2.2	Average Particle Displacement	43
4.3	Performance Evaluation for Assistive Grouser Model.....	46
4.3.1	Normal Force of Grouser Surface	47
4.3.2	Grouser Translation Destructive Area	49
CHAPTER 5		51
CONCLUSION		51
5.1	Introduction	51
5.2	Simulation Conclusion for Conventional Rover and Modified Rover	51
5.3	Assistive Grouser Model	52
5.4	Future Work.....	52
References.....		52



CHAPTER 1

INTRODUCTION

This chapter presents the research overview, research motivation, research problem statement, research objectives, research scopes, research contribution, and thesis organization/outline.

1.1 Research Overview

Today, there is an increasing need for mobile robots which are able to perform tasks that cannot be done by a human because the task is too dangerous or maybe the task is out of human capability. For example, two Soviet mobile robot vehicles, the Lunokhods, have landed on the moon in November 1970 and in January 1973. Its task was to measure the physical and chemical properties of the lunar soil [1]. One type of mobile robot that has been designed is wheeled rover mobile robot. Usually, this type of wheel rover robots was used for driving over rough terrain as the example above. The performance of wheeled rovers has become the focus of study by many researchers in order to improve the mobility performance of the robot.

Recently, the focused issue is on improving the mobility performance on one of the most challenging terrains to traverse for the outdoor wheeled rover; the unconsolidated sandy incline. Research on mobility performance is important to prevent mobility failures. As an example, if a rover was sent for planetary exploration and experiences mobility failures during one of its tasks, human assistance might not be possible, especially if it is on a distant planet. One of the famous cases of wheel rover challenge is the NASA “Spirit” Mars rover. During its task, “Spirit” Mars rover was embedded into the sand and unable to move forward when moving on a sandy slope in 2009 [2]. All extrication plans to free it has failed. Its twin

rover “Opportunity” was also immobilized and the wheel sunk into the sandy terrain but it managed to recover from getting stuck in the Purgatory Dune in 2005 after 5 weeks of continuous effort [2]. Efforts to improve mobility on sandy slope have been made.

Ibrahim, A.N., et al. built a new prototype design of wheeled rover by attaching an “assistive grousers” to the wheel of the rover. The function of this assistive grouser mechanism is to aid the wheeled mobility on soft sand terrain. An experimental test was successfully carried out and the comparison data regarding the effectiveness of conventional wheel rover and modified wheel rover was recorded. Conventional wheel rover refers to a wheel that attaches with “fixed grousers” while modified wheel rover refers to a wheel that attaches with “assistive grousers”.

During the experimental test, both conventional wheel rover and modified wheel rover has been tested using different length of grousers at different sand inclination angles. The result shows that, with the use of the assistive grousers, the performance of wheel rover more effective because at the end of the experiment modified wheel rover able to traverse all the tested sand surface inclination (0, 10, 20 and 30 degrees) with lower level of sinkage as the length of assistive grousers increase. Compared to conventional wheel rover, the increasing of fixed grouser’s length did not assist the rover to climb the stepper sand surface inclination. For 30 degrees sand surface inclination, conventional wheel rover failed to climb the slope. Besides that, the average current consumption and the volume of sand displacement behind the wheel for modified wheel rover that was recorded at the end of the experiment was smaller compare to the data recorded for conventional wheel rover.

Based on Ibrahim, A.N., et al. discussion from the previous study, for the conventional wheel rover, the amount of sinkage increased when there is not enough traction force generated. And as the wheel continues to rotate, it lifted sand from below the surface increasing sinkage and the sand accumulated behind the wheel [3]. For the modified wheel rover, it generated a large amount of traction force during the grousers movement and exit the sand surface when the grousers movement without displacing large amount of sand behind the wheel. Figure 1.1 and Figure 1.2 shows conventional wheel rover and modified wheel rover on a level incline.

Figure 1.1 shows the fixed grouser (labeled as B) and wheel for conventional wheel rover on a level inclination. It is able to gain traction to move forward from the grouser movement between the points of grouser entry into the sand (OY) to the vertical line (OG)

which directs force W downwards pushing the sand and stiffening the local sand region. The grouser movement from OG to the point where the grouse exits the sand (OZ) directs force X upwards, pushing the sand below the wheel upwards and lifting it toward the surface. Figure 1.2 shows the assistive grouser that attached to the shaft (labeled as A) for modified wheel rover on a level inclination. The grousers rotate in sync as the shafts are mechanically connected to one another. If the assistive grouser angle is set so as to maintain an angle parallel to the direction of the gravitational force as the wheel turns, the OG - OC grouse movement does not lift any sand towards the surface, reducing the amount of sand accumulated behind the wheel.

But, during the experiment, the interaction between the grousers and the sand cannot be observed and recorded. Because of that, in this research study, a simulation modelling for the experiment above will be carried out. By this simulation, the contact interaction between the grousers and the sand can be estimated and can be analyzed. The analysis of the interaction will show how the modified wheel rover with assistive grousers can successfully solve the problem of sinking wheel. Thus, this simulation result will validate the hypothesis conclusions derived from the recorded experimental result which is modified wheel rover more effective compared to conventional wheel rover because modified wheel rover managed to climb the inclination slopes without displacing large amount of sand behind the wheel with small current consumption and small maximum angles sinkage.

In this simulation modelling, a method known as Discrete Element Method (DEM) will be used. DEM is a numerical method for modelling the dynamics of solid particles [4]. It shows the interaction of particles with each other at discrete contact point. The explanation about DEM will be discussed in Chapter 2 subchapter 2.2. The parameters that will be used in the simulation modelling for the wheel rover model and particles model will be future explained in Chapter 3 subchapter 3.2.

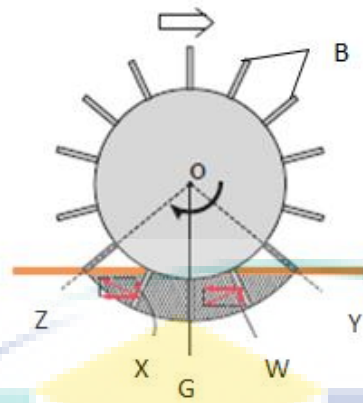


Figure 1.1: Conventional wheel rover on a level inclination [3]

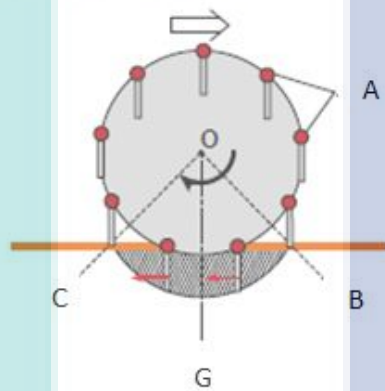


Figure 1.2: Modified wheel rover on a level inclination [3]

1.2 Research Motivation

The invention of mobile robots has become one of the biggest help for a human. Mobile robots can do the task that cannot be done by human either the task is too dangerous or maybe it is out of human capability. For example, mobile robot was used to examine critical infrastructures, to search for missing persons driven underwater by the tsunami, to remove fragment in the disaster sites, and to examine buildings that were in danger of collapsing. Wheeled rover robot is a vehicle that usually used for driving over rough terrain. Wheel rover robot was usually chosen instead of continuous tracks because wheel rover robot is lightweight compared to continuous tracks. That is the main reason why wheels are used especially in cases when the mass of the robot is a critical property as an example for planate exploration research.

Another example the use of wheel rover is for radiation monitoring. Japan Atomic Energy Agency (JAEA) developed a gamma-ray camera (J-3 with γ eye – Figure 1.3) which is based on RESQ-A. It was developed in year 1999 after the disastrous nuclear accident in Tokaimura [5]. J-3 was used to monitor gamma rays in reactor building 2 on 23 September 2011 [6].

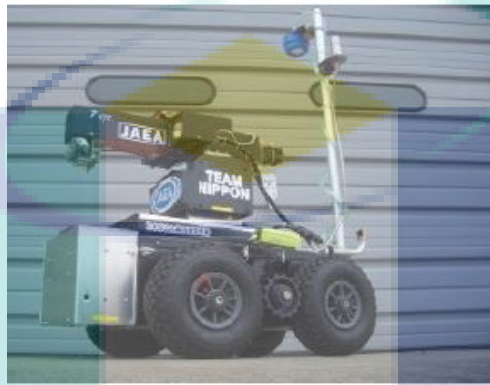


Figure 1.3: Remotely controlled robot J-3 with γ eye camera [6]

Researchers come out with new ideas in order to improve the mobility performance of the wheel rover especially for challenging terrains such as unconsolidated sandy incline. For example, Nakashima, H., et al. reported in his paper that when the height and number of the grouser that attached to the wheel increase, the gross traction and running resistance during slope locomotion will also increase [7]. While Sutoh., M., et al. reported that when the rover weight increase, its traveling performance will decrease and the mobility can be improve effectively by installing grousers on the wheel compare to increasing the wheel diameter and width [8].

Ibrahim, A.N., et al. come out with a new idea of grouser which is “assistive grousers” that was attached to the side of the conventional wheel rover. During the experimental test, two types of rovers have been tested which is conventional wheel rover (attached with fixed grousers) and modified wheel rover (attached with assistive grousers). These two types of rovers were tested on an indoor sand incline at different angles of sand surface inclination. With this assistive grousers help, the modified wheel rover managed to climb the unconsolidated sandy incline at 30 degrees sand surface inclination without the wheel stuck into the sand while conventional wheel rover unable to climb the unconsolidated sandy incline at 30 degrees sand surface inclination. However, during the experimental test, the interaction between the grousers and the sand cannot be directly measured.

Because of that, in order to investigate how the assistive grouser interacts with the sand and managed to climb the sand surface inclination slope, a simulation modelling will be carried out. By modelling the simulation, the movement of the sand particles below the rotating wheel can be observed and recorded. It is hoped that it will explain how the sand particles moved from under the conventional wheel rover and accumulate behind the wheel causing the wheel stuck into the sand. And it is hoped that it will explain how the assistive grousers prevent the modified wheel rover from getting stuck into the sand by exit the sand surface during grouser movement without displacing large amounts of sand.

This simulation modelling will validate the conclusion of the previous study by Ibrahim, A.N., et al. which is modified wheel rover is more effective compared to conventional wheel rover because of the different sand flow under the wheel. At the end of the previous study, the result shows that at 30 degrees sand surface inclination slope, modified wheel rover managed to climb the slope but conventional wheel rover unable to climb the slope. A hypothesis has been made to explain the failure of conventional wheel rover at the end of the experiment. It was stated that conventional wheel rover generated not enough traction force causing the amount of slip to increase. As the wheel continues to rotate, it lifted sand from below the surface increasing sinkage and sand accumulated behind the wheel [3]. But for modified wheel rover, it generated a large amount of traction force during grouser movement and the grouser exit the sand surface during grouser movement without displacing large amount of sand and prevents the sand move to the back of the wheel and accumulated behind it.

1.3 Problem Statement

Lightweight wheeled rover has a high risk of getting stuck in the unconsolidated sand terrain because when slippage occurs the wheels tend to sink into the sand. To solve this problem, Ibrahim, A.N., et al. purposed a new design of wheel by using “assistive grousers”. These assistive grousers were attached to the side of a conventional wheel rover in order to minimize sand movement and subsequent sinkage [3]. During the experiment, two types of wheel rover which are conventional wheel rover and modified wheel rover was tested and the result was compared. Conventional wheel rover refers to a wheeled rover that attached with fixed grousers. Modified wheel rover refers to a wheeled rover that attached with assistive grousers. Both wheel rovers were tested to climb sand surface inclination slope at different angles by using different length of grousers. At the end of the experiment, it recorded that,

modified wheel rover successfully climbed 30 degrees sand surface inclination slope by using 90 mm assistive grouser length, but conventional wheel rover unable to climb the slope although by using 80 mm fixed grousers.

From the experiment observation, when the modified wheel rover managed to climb the 30 degrees sand surface inclination slope, maximum sinkage angle that produced was small compared to conventional wheel rover. The current consumption produced by modified wheel rover also small when it is compared with conventional wheel rover. From the result obtained, it shows that modified wheel rover more effective compared to conventional wheel rover. During the previous study, it was hypothesized that the effectiveness of modified wheel rover because of the interaction between the assistive grousers and the sand. When the assistive grousers moved it generated a large amount of traction force. Then, the grousers exit the sand during the grouser movement without displacing large amount of sand. Because of that, it was able to climb the inclination slope. But, for the conventional wheel rover, the amount of slip increase when there is not enough traction force and as the wheel continues to rotate, it lifted the sand from below the surface increasing sinkage and the sand accumulated behind the wheel. Because of that, the wheel sunk into the sand and failed to climb the inclination slope.

However, during the experiment, the contact interaction between the grousers and the sand cannot be directly measured because from the experiment, only the rough movement interaction can be observed. Based on the experimental test alone, it cannot be verified how the modified wheel rover and the sand interact with each other that make modified wheel rover become more effective compared to conventional wheel rover. Experimental test only used a limited number of parameter sets due to time and hardware restraints.

Thus, in this research study, a simulation modelling will be carried out. In this simulation, the interaction between the grousers and the sand can be modelled using available terramechanics models and from the results, parameters such as sand flow below the rotating wheel can be observed through the simulation modelling. The simulation result will then be used to investigate how and why modified wheel rover is more effective compared to conventional wheel rover on inclination slope. The experimental data that was recorded will be used to validate the simulation modelling data. The simulation result will be used to validate the hypothesis (as mention above) from the previous study.

1.4 Research Objectives

The goal of this research study is to investigate the effect of grousers to sand-grouser interaction by simulation modelling. To achieve this goal, there are several objectives which are as follow:

- i. To design a 3D simulation of sand flow under a rotating wheel using Discrete Element Method (DEM) for conventional wheel rover (attached with fixed grousers) and modified wheel rover (attached with assistive grousers).
- ii. To propose a model for assistive grouser movement when attached to a wheel.
- iii. To validate the conclusions derived from previous experimental data through simulations.

1.5 Research Scopes

In order to overcome the problem of wheel that stuck in an unconsolidated sand terrain, researchers have come with a different kind of modification wheel. For example, one of the researchers has purpose to attach an “assistive grousers” to the wheel to solve the problem [3]. The researcher carried out an experimental test using a prototype rover. The test was conducted for a conventional wheel rover (attached with fixed grousers) and a modified wheel rover (attached with assistive grousers). And the experiment shows that the modified wheel rover was more effective compared to conventional wheel rover.

From the data recorded, modified wheel rover managed to climb 30 degrees sand surface inclination slope by using 90 mm grouser length. And at that angle, smallest maximum sinkage angle was recorded. It also produced small current consumption. For conventional wheel rover, it failed to climb at angle 30 degrees sand surface inclination slope even though by using the longest grouser length which is 80 mm. At angle 20 degrees, conventional wheel rover already produced maximum sinkage angle. The current consumption also high compared the modified wheel rover. These situations happen because the sand-grouser interactions for conventional wheel rover and modified wheel rover are different.

So based on the previous experimental study, a simulation modelling will be carried out in this study in order to investigate the sand-grouser interaction and the simulation result will be validated by the experimental result. Therefore, the scopes of this study are:

- i. Design conventional wheel rover (attached with fixed grousers) and modified wheel rover (attached with assistive grousers) model for simulation.
- ii. Run the simulation of rover (conventional and modified) by using DEM simulator.
- iii. Validate the simulation result with the experimental result.
- iv. Verify conclusions of previous study regarding 2-dimensional flow of sand during wheel rotation.

1.6 Research Contribution

This research focused on the design of a simulation model from the previous experiment parameters. The purpose of this simulation is to investigate the interaction between the wheel's grousers and the sand particles when the wheel moving on the sand slope. The main contributions of this research study are:

- i. Observation on sand-grouser mechanics interaction when using assistive grouser.
- ii. Analysis of parameters that effect wheel performance when climbing sand surface inclination slope.
- iii. A new model that estimates the flow of sand and the generated force by the assistive grouser system.

1.7 Thesis Organization/Outline

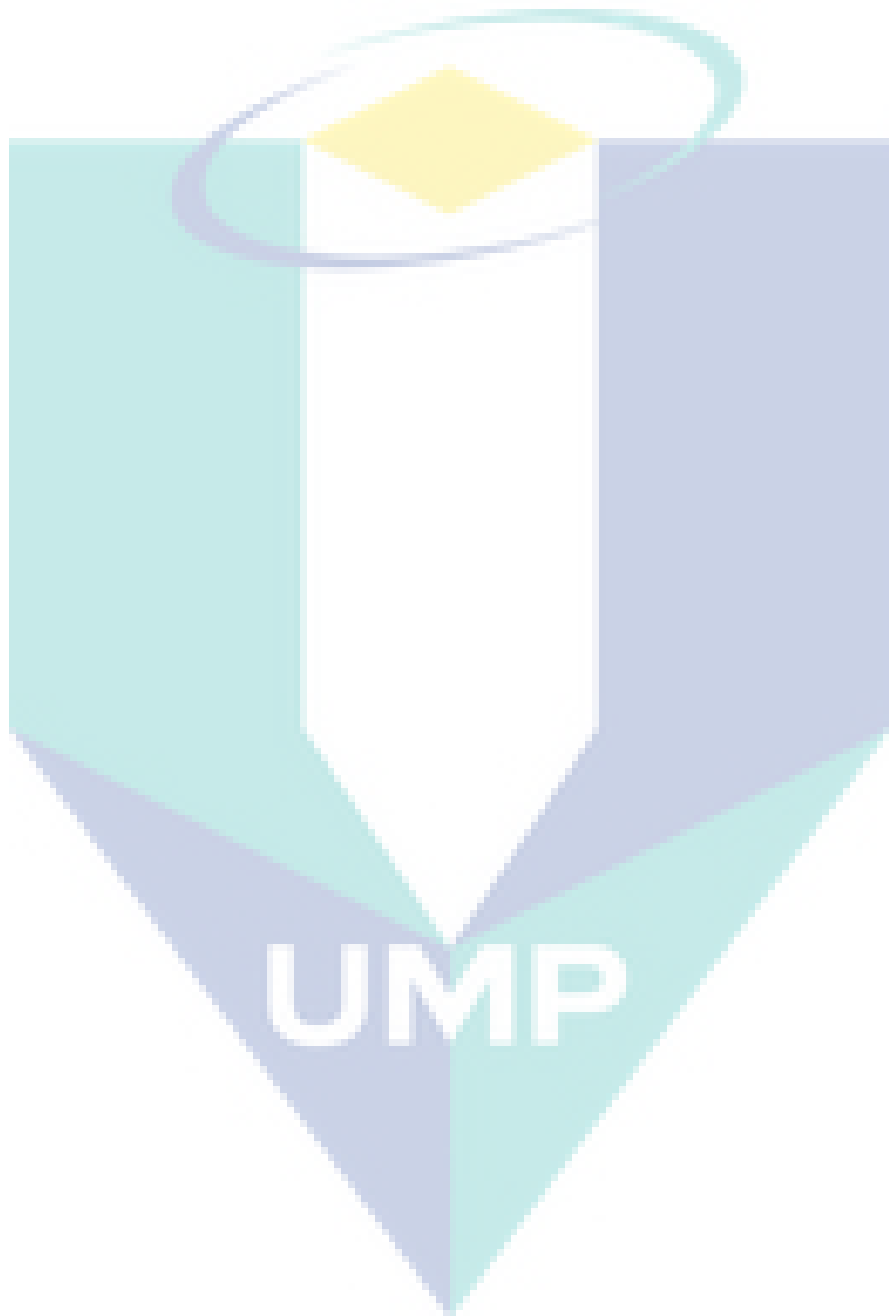
This thesis is organized as follows:

Chapter 2 of this thesis will review the literature review of this study. It will discuss the Discrete Element Method (DEM), previous works that using DEM, terramechanics modelling and referred case study.

Chapter 3 will consist of research methodology. This chapter will portray the research methodology process flow and the research components.

Chapter 4 of this thesis will discuss the result of the simulation as well as the analysis of the result. In this chapter, it will also discuss the experimental test result validation.

For the last chapter which is **Chapter 5**, it will conclude the findings and observations of this research study. And provide recommendations for future work which can be done by future researcher.



CHAPTER 2

LITERATURE REVIEW

2.1 Introduction

This chapter presents the knowledge of Terramechanics Modelling, Computational Fluid Dynamics (CFD), Finite Element Method (FEM), and Discrete Element Method (DEM). Next, it discusses the related study of previous work that using DEM. Lastly, in this chapter, it presents the discussion from a referred case study by Ibrahim, A.N., et al.

2.2 Terramechanics Modelling

Terramechanics is a study of soil properties specifically the interaction of wheeled or tracked vehicles on a various surface. Smith, W.C. state [9] that the field of terramechanics studies the interaction between machine and terrain. Terramechanics methods can aid the design and operation of small vehicles to help ensure they do not become immobilized due to limited traction or energy depletion [10]. It is important for steady-state and dynamic operation. This terramechanics field began to develop as a result of the interest in land locomotion mechanics generated by the pioneering work of Dr M.G. Bekker [11].

There are three types of terramechanics modelling which is by using Bekker method, dynamic Bekker method, and Discrete Element Method (DEM). Bekker method characterizes the semi-empirical terramechanics models. By using this method, many soil coefficients can be determined through simple soil tests and computationally efficient compared to other methods. But it only describes steady-state relationships, not dynamic equations and limiting its applicability for transient operation, for example, multi-body vehicle simulations. Beside that the soil dynamic is not considered and limited in modelling more complex interaction.

Dynamic Bekker method addresses two limitations of Bekker method which is multi-body dynamics and complex soil profiles. By using this method, the wheel is treated as a free body with inertia. The soil is discretized so the Bekker stress equations can be applied to each region. For DEM, the soil is modeled as a granular material made of many particles and each particle is capable of free body motion. DEM is flexible simulation method not limited to wheel-terrain and it discrete nature ideal for granular soils.

The comparison between this three methods has been discussed by Smith, W., et al. [10]. Smith, W., et al. reported that DEM produced more accurate wheel performance for

both quantitatively and qualitatively, compared to Bekker method and dynamic Bekker method. The accuracy came with a large penalty in computation effort and efficiency. DEM has significantly greater simulation capabilities compared to both Bekker methods [10]. Thus the scope of this study is by using 2D DEM as a modelling method and analysis.

2.3 Computational Fluid Dynamics (CFD)

Computational Fluid Dynamics or CDF modelling is processes that apply for resolving different fluid flow. For example, the problem that related to flow of velocity, density, temperature and chemical concentrations for any area where flow is present. It is a numerical method to calculate non-linear differential equations that relate to fluid flow. CDF provides a qualitative (sometimes quantitative) prediction of flows by mathematical modelling (partial differential equations), numerical methods (discretization and solution techniques) and software tools (solvers, pre and post processing utilities). The industries that relate to CFD analysis are aerospace/aeronautics, automotive, building HVAC (heating, ventilation and air conditioning), chemical/petrochemicals, and etc.

Researchers began to use CFD program because the main advantage is it uses full Navier-Stroke equations and provides a solution to the flow problem, while finite difference codes are based on the Reynolds equation. Three-dimensional computational fluid dynamics (3D-CFD) was used to analyze the performance characteristic of a hydrodynamic journal bearing lubricated with a Bingham fluid. To calculate the hydrodynamic balance of the journal using “dynamic mesh” technique, the FLUENT software package was used. The result obtained from the 3D-CFD model was fit with the experimental and analytical data from the previous investigation on Bingham fluids [12].

The influence of end seal clearance and flow path length on the performance of a circular orbiting squeeze film damper with a central circumferential feed groove was studied by Chen, P.Y.P. and E.J. [13] using CFD package CFX4.2. Ranjan, V., R. Pai, and D. Hargreaves [14] used the CFD approach to model fluid flow in a journal bearing with three equally spaced axial grooves which were supplied with water from one end by using FLUENT. It also calculated the stiffness and damping coefficients.

2.4 Finite Element Method (FEM)

Finite Element Method (FEM) or Finite Element Analysis (FEA) is a numerical method for solving engineering and mathematical physics problems. The problems include structural analysis, heat transfer, fluid flow, mass transport, and electromagnetic potential. In addition, FEM is useful for problems with complicated geometries, loadings, and material properties where analytical solutions cannot be obtained. The common application that involves FEM analysis are mechanical/aerospace/civil/automotive engineering, structural or stress analysis, fluid flow, heat transfer, electromagnetic field, biomechanics and etc.

For mechanical engineering field, FEM was widely used to design the automobile parts such as the lightweight design of automotive frame and the analysis of the body vibration characteristics. The analysis can effectively solve the problem of the whole deformation and stress distribution of complex parts. Besides that, FEM used to analyze the strength and stiffness of the transmission shell, suspension systems, brake systems, wheels, and other auto parts. FEM also used to analyze stress condition under different working conditions, which effectively improves the design efficiency and reduces the calculation error [15].

Silva, E.P.d., F.M.d. Silva and R.R. Magalhães [16] used FEM in their study to analyze the stresses and displacements of a coffee harvester structure for static simulation. The study covers the static analysis on the structure of a machine coffee harvester by considering two situations which are machines with rear wheels aligned and misaligned. By using FEM, it was possible to generate values of stresses and displacements for both situations. The result obtained shows the suitable design for structural components of a machine coffee harvester.

2.5 Discrete Element Method (DEM)

Discrete (or distinct) Element Method (DEM) was initially proposed by Cundall [17]. DEM is a numerical method for modelling the dynamics of solid particles which interact with each other at discrete contact point [4]. It is a well-known computational tool for dynamics of particles or powders in science and engineering [7]. Nakashima, H., et al. discuss in his paper [7], DEM is based on equation of motion where all forces such as contact reaction and body forces acting on the element of interest were added to the force term. The DEM solution is generally based on an explicit integration whose stability was conditional which implies that

the time step should be as small as possible [17]. In DEM simulations, at every numerical iteration time step, the properties of a stressed assembly of rigid spherical particles such as position, velocity and contact forces were updated. The translational and rotational displacements for each particle was obtained based on Newton's second law of motion equation [4].

Nakashima, H. and T. Kobayashi utilized DEM as a computational tool in order to analyze soil-wheel interactions in terramechanics. In their study, it used circular shape elements to model individual grains of soil, primarily to reduce the computational time [18]. The shape of discrete element can be freely determine. But a simple shape such as 2D circle or 3D sphere is widely used in term of the detection of contact [7, 17-19]. In order to minimize computation time while maximizing the number of DEM elements used in the simulations within the constrains of available computation resources, 2D DEM was chosen instead of 3D DEM as has been designed by Nakashima, H. and T. Kobayashi in their study [18].

2D DEM was commonly used by researchers for the simulation model. As an example, 2D DEM has been used by Khot, L.R [20] and Nakashima, H., et al. [7] to simulate the running behaviors of a rigid wheel on sandy soils or granular lunar soil. DEM shows an advantage to simulate a model for sand, soil or rock. Other element shapes have been applied in 2D DEM in the past previous study. For example, an ellipse [21], polygon [22] or a clump of two or more circles [23].

2.6 Previous Works using Discrete Element Method (DEM)

This section will discuss the previous researcher's works that using Discrete Element Method (DEM) in their simulation model. Smith, W., et al. [10] do comparison and evaluation between DEM and traditional modelling methods which is Bekker method and dynamic Bekker method for simulating steady-state wheel-terrain interaction for small vehicles. This three common terramechanics methods were compared based on the performance of a small wheel driving on Mojave Martian Simulant at steady state. The evaluations were made based on quantitative and qualitative, and computational efficiency.

At the end of the simulation, the result shows that DEM provided the best fit of the experimental result. For Bekker method, it has similar results as DEM for large positive and negative slip ration but the error is significantly large near zero slip. This study gives a better understanding of the advantages and disadvantages of each method and a direct comparison of prediction accuracy.

Nakashima, H. and T. Kobayashi investigate the effect of gravity on rigid wheel sinkage, motion resistance, and slip [18]. The result was used to evaluate the finding in Wong and Kobayashi [24]. In this study, 2D DEM was used instead of 3D DEM to minimize computational time and maximizing the number of DEM element in the simulation. And, to reduce the computational time, circular elements were used to model the individual soil. At the end of the research, the result that obtained by using 2D DEM substantiate all the findings presented by Wong [25] and by Wong and Kobayashi [24].

Nishiyama, K., et al. carried out a study to extend the applicability of previous developed 2D FE-DEM code for elastic deformable wheels [26]. The accuracy of the analysis was compared with the experimental result of prototype wheel (ESA Martian rover) [27]. In the simulation program, a coupling method was used which is Finite Element Method (FEM) and Discrete Element Method (DEM). FEM was used to model the wheel and DEM was used to model the soil. At the end of the study, the result shows similar behaviours of tractive performance as recorded in the experimental result for gross tractive effort, net traction, running resistance, and wheel sinkage. The previous development of 2D FE-DEM for application to tractive performance analysis of the elastic flexible wheel was upgraded in this study where a new algorithm learned from PIC-controller model was introduced.

Di, S., et al. [28] design a simulation model to investigate the effects of model size and particle size on the simulated microscopic mechanical properties, uniaxial compressive strength, Young's modulus, and strength of sea-ice sample, using Discrete Element Method (DEM) with bonded-particle model. The result from the simulation shows that model size and particle size in discrete element simulations has an effect on the response of the sample. It was recorded that the response of fine sample has large value compared to coarse sample.

Zhao, C.-L. and M.-Y. Zang, study the application of FEM/DEM and alternately moving road method to the simulation of tire-sand interactions (AMRM) [19]. The purpose of this study was to apply the three-dimensional FEM/DEM to the simulation of tire-sand interactions and purpose the AMRM to improve the possibility of engineering applications.

In this simulation, FEM/DEM possessed the ability to analyze the complex character of the tire through the FEM and simulate the granular features of sand through DEM. AMRM was used to control the model size and to improve the computational efficiency for the simulation of the arbitrary length of the road. At the end, it was concluded that the comparison between simulation results and reported results show that FEM/DEM was straightforward and effective tool to investigate the behaviors of tires when traveling on sand.

From the previous studies, it shows that DEM is a method that commonly used by researchers to model small particles such as sand, soil or rock. 2D is a common shape that has been used by researchers because it can minimize the computational time and maximize the number of DEM elements used in the simulation. Thus, for this research study, 2D circle shape will be used to model the sand particles by using DEM.

2.7 Referred Case Study

Ibrahim, A.N., et al. built a new prototype design of wheeled rover to improve the mobility performance of wheeled rover for outdoor unconsolidated sandy incline. The new prototype design of wheeled rover was attached with assistive grousers. The objective of the experiment was to purpose a concept of using an “assistive grousers” that attached to the side of a conventional wheel rover in order to minimize sand movement and subsequent sinkage [3]. During the experiment, two types of wheeled rovers were used which is conventional wheel rover and modified wheel rover. Conventional wheel rover refers to a wheel that attached with “fixed grousers” while modified wheel rover refers to a wheel that attached with “assistive grousers”. The result for both rovers was compared.

2.7.1 Wheeled rover mechanism

Two types of wheel rovers were used in Ibrahim, A.N., et al. experimental test which is conventional wheel rover and modified wheel rover. Table 2.2 below shows the mechanism of wheeled rover used for the experiment. Figure 2.1 and 2.2 shows the model of conventional wheel rover (attached with fixed grousers) and modified wheel rover (attached with assistive grousers).

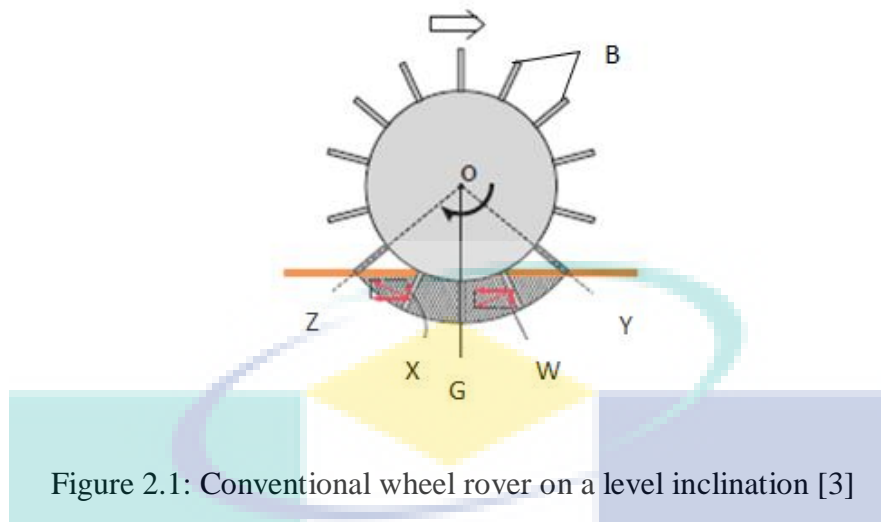


Figure 2.1: Conventional wheel rover on a level inclination [3]

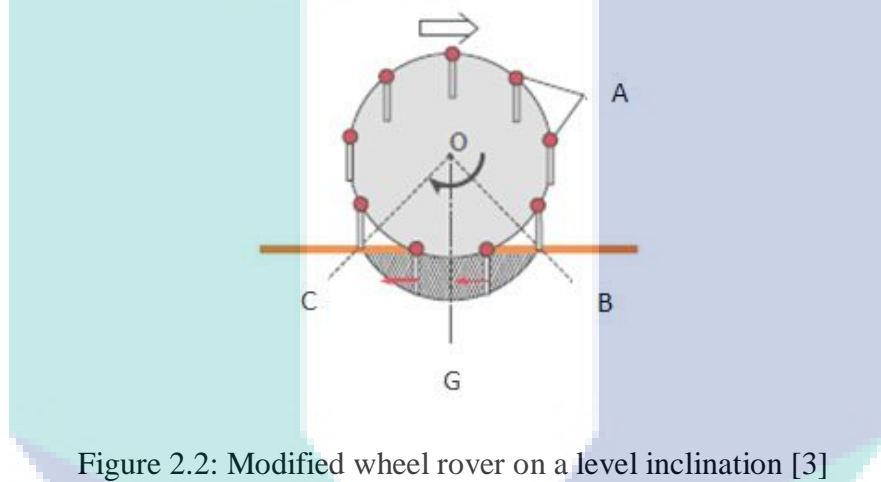


Figure 2.2: Modified wheel rover on a level inclination [3]

Figure 2.1 shows the fixed grouser (labeled as B) and wheel for conventional wheel rover on a level inclination. It gains the traction force and able to move forward from the grouser movement between the points of grouser that enter the sand (OY) to the vertical line (OG) which directs force W downwards pushing the sand and stiffening the local sand region. The movement of grouser from OG to the point where the grouser exits the sand (OZ) directs force X upwards, pushing the sand below the wheel upwards and lifting it toward the surface. Figure 2.2 shows the assistive grouser that attached to the shaft (labeled as A) for modified wheel rover on a level inclination. As the shafts are mechanically connected to one another the grousers rotate in sync. The OG-OC grouse movement does not lift any sand towards the surface if the assistive grouser angle is set to maintain an angle parallel to the direction of the gravitational force as the wheel turns. Besides that, it reducing the amount of sand accumulated behind the wheel.

Table 2.2: Wheeled rover mechanism

	Conventional wheel rover	Modified wheel rover
Type of grouser used	Fixed grousers	Assistive grousers
Grouser length (mm)	20, 40,60 and 80	50, 70 and 90
Absolute angle ϕ_a	-	60° forward and backward relative to the gravitational force direction.
Sand surface inclination angles (degree)	0 (level inclination), 10, 20 and 30	0 (level inclination), 10, 20 and 30
Testing field	Indoor sand incline using Toyoura sand	
Data recorded	Maximum sinkage angle, sand displacement volume, slip ratio and average current consumption (over five runs)	

Table 2.1 shows the mechanism for conventional wheel rover and modified wheel rover. In the experimental test, the grouser length used for conventional wheel rover in the testing field is 20, 40, 60 and 80 mm. While the grouser length used for modified wheel rover in the testing field is 50, 70 and 90 mm. Both conventional wheel rover and modified wheel rover was tested on 0 (level inclination), 10, 20 and 30 degrees of sand surface inclination angles. The sand used for the experiment is Toyoura sand. The sand box was built from wooden boards and steel frames. Toyoura sand was filled in the box about 0.725 m³ in a uniform depth of 250 mm across the surface area, making the total weight 900kg. Toyoura sand was chosen as a test medium because of its homogenous properties that well represent unconsolidated sand terrain [3]. The mobility test was carried out for five times and during steady running state of the rover, maximum sinkage angle, sand displacement volume, slip ratio, and average current consumption was recorded.

2.7.2 Mobility testing set up

To measure the performance of the rovers (conventional wheel rover and modified wheel rover), indoor sand incline mobility test field was used as shown in Figure 2.3.

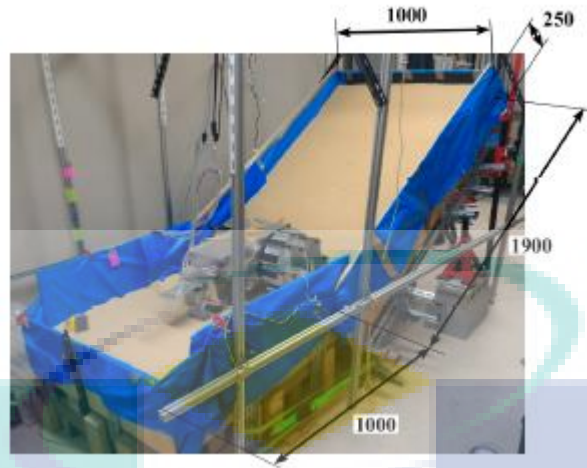


Figure 2.3: Indoor sand incline mobility test field (30 degrees sand surface inclination) [3]

Figure 2.3 above shows the starting point for the rover. It was at the end of a 1000 mm long level surface at the foot of the incline. Then, the rover starts to climb on the 1900 mm incline surface. The mobility test stop after the rover touched the board at the top of the incline. The data was recorded when the rover reaches a steady running state. The mobility testing performance criterion was based on maximum sinkage angle, sand displacement volume, slip ratio, and average current consumption.

2.7.3 Result after mobility testing

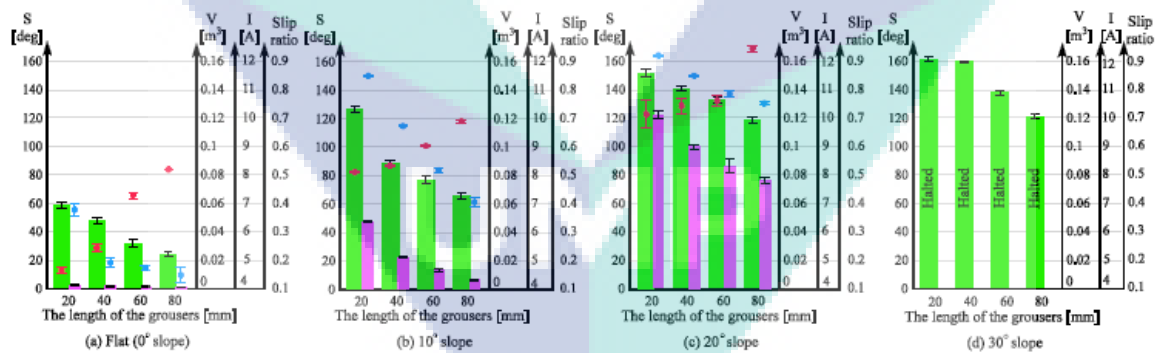


Figure 2.4: Mobility test result for conventional wheel rover on sand surface inclination; (a) 0 degree; (b) 10 degree; (c) 20 degree; (d) 30 degree [3]

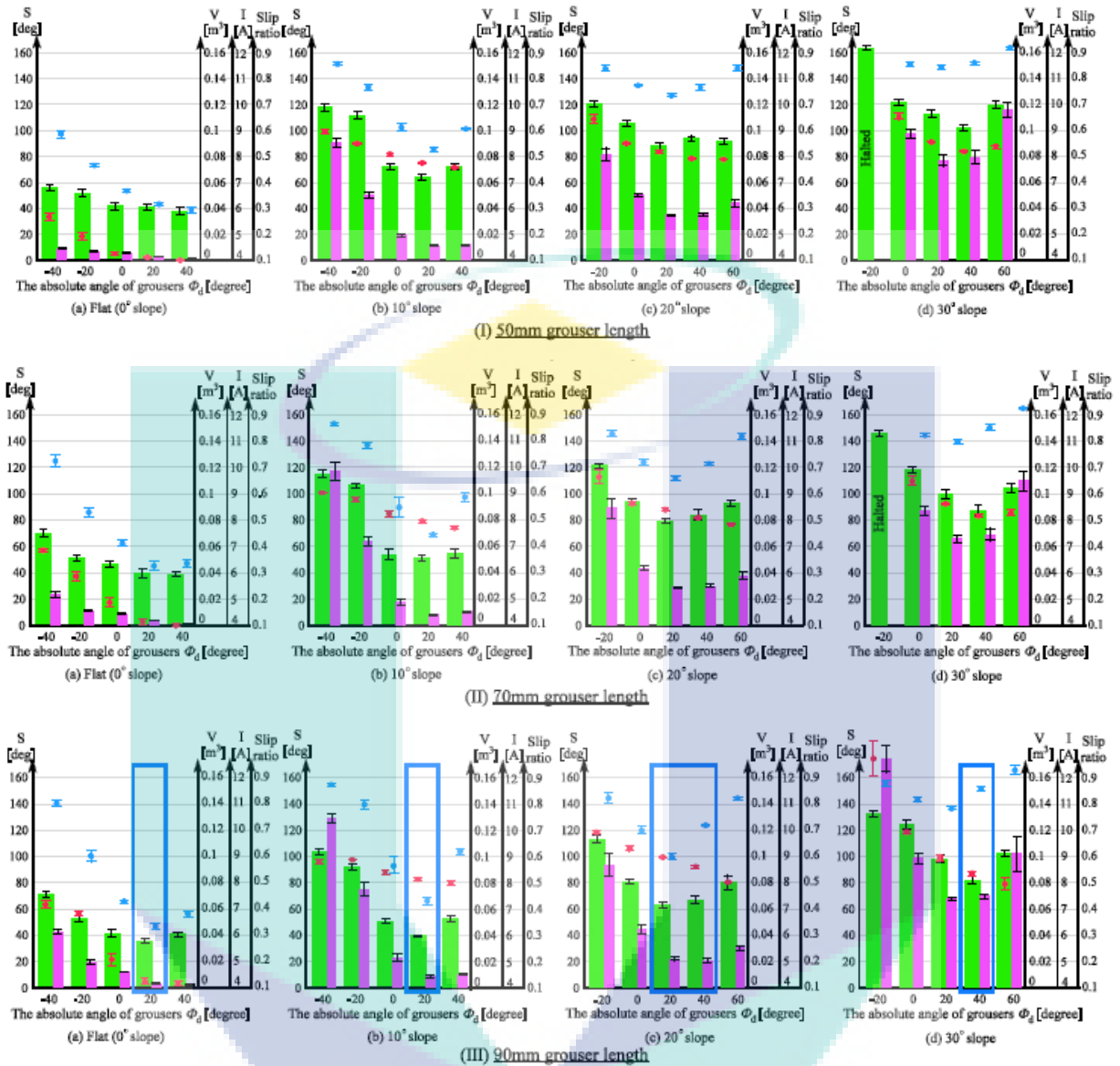


Figure 2.5: Mobility test result for modified wheel rover on sand surface inclination angle; (a) 0 degree; (b) 10 degree; (c) 20 degree; (d) 30 degree with grouser length; (I) 50mm; (II) 70mm; (III) 90mm [3]

Figure 2.4 shows the mobility test result for conventional wheel rover on sand surface inclination while Figure 2.5 shows the mobility test result for modified wheel rover on sand surface inclination. For both figures, green bar represents as maximum sinkage angle, the pink bar represents as sand displacement volume per one meter of distance traveled, the black dot represents the slip ratio and the red dot represents the average current consumption.

For 30 degrees sand surface inclination angles, the conventional wheel rover unable to climb the inclination slope but modified wheel rover successfully climbed the inclination slope. Modified wheel rover (blue rectangle in Figure 2.5 III d) with 90 mm assistive grouser

length and the angle ϕ_d was 40 degrees forward shows the smallest sinkage angle which is 82 degrees during steady running. Besides that, the average current consumption was measured during the experiment which is 8.36 A for modified wheel rover, significantly less than conventional wheel rover which is exceeded 20 A.

For 20 degrees sand surface inclination, the conventional wheel rover exhibited maximum sinkage angle which is over 118 degrees regardless of the rover's configuration. But modified wheel rover in the optimal configuration as shown in Figure 2.5 IIIc (assistive grouser 90 mm, ϕ_d 20 and 40 degrees) the maximum sinkage angles observed were 63 degrees and 67 degrees. It shows an obvious improvement. The smallest sand displacement volume for conventional wheel rover was 0.076 m^3 for a fixed grouser length 80 mm but the sand displacement volume for modified wheel rover in the optimal configuration (Figure 2.5 IIIc) was only 0.022 or 0.21 m^3 . As for the comparison of average current consumption, conventional wheel rover showed a minimum average current consumption of 10.1 A for 20 mm fixed grouser length. But modified wheel rover (Figure 2.5 IIIc) consumes a little average current consumption which is 8.6 or 9.0 A in the optimal configuration.

For 10 degrees sand surface inclination, the optimal configuration (Figure 2.5 IIIb) with assistive grouser length 90 mm and ϕ_d 20 degrees forward, showed a maximum sinkage angle of 40 degrees. It is much smaller than the maximum sinkage angle of 66 degrees for conventional wheel rover with 80 mm grouser length. In addition, the average current consumption for modified wheel rover (Figure 2.5 IIIb) was 8.14 A at the optimal configuration. It is smaller than any values measured for the conventional wheel rover (Figure 2.4b).

For 0° (level surface inclination), the optimal configuration (Figure 2.5 IIIa) with assistive grouser length 90 mm and ϕ_d 20 degrees forward showed the maximum sinkage angle of 36 degrees and 0.0037 m^3 sand displacement volume for modified wheel rover. It is inferior to the best result achieved for conventional wheel rover (Figure 2.4a) with sinkage angle 24 degrees and 0.0009 m^3 sand displacement volume. However, the 36 degrees of maximum sinkage angle is still considered small and the difference in the probability of entering the "stuck" stage is not considered. The average current consumed by conventional wheel rover with 80 mm fixed grouser length was 8.19 A. It is almost double the average current consumed by modified wheel rover at optimal configuration (Figure 2.5 IIIa) which is 4.24 A.

2.7.4 Discussion and conclusion for mobility testing

From the result obtained, that modified wheel rover shows the best performance for all sand surface inclination angles by using 90 mm assistive grouser length. The angle of assistive grouser relative to the gravitational force direction ϕ_d that produced the best performance was 20 degrees for a 0-10 degree inclination, 20-40 degrees for a 20 degrees inclination angle and 40 degrees for a 30 degrees inclination angle. The wheeled rover able to travel on all soft sand surface inclination by using the assistive grousers of length 90 mm and the angle of ϕ_d according to the angle of inclination the rover is traversing. Modified wheel rover consume a small average of current, generated less torque output to rotate the wheel and reduced the size of the actuator.

The amount of slip was reduced when there is enough traction force generated to compensate for the force of gravity component parallel to the incline surface. Thus the rover is able to climb the sand surface inclination with minimal sinkage. The amount of slip for conventional wheel rover increased because it generated not enough traction force and as to wheel continues to rotate, it lifted the sand from below the surface increasing sinkage and the sand accumulated behind the wheel. For modified wheel rover, during the grouser movement it generated a large amount of traction force and exits the sand surface without displacing a large amount of sand.

From the experiment that has been carried out by Ibrahim, A.N., et al., it can be concluded that the modified wheel rover able to traverse all the tested sand surface inclination (0, 10, 20 and 30 degrees) with lower levels of sinkage as the length of assistive grousers was increased. But for conventional wheel rover, by increasing the length of fixed grousers it did not assist the rover to climb the steeper sand surface inclination and it could not even traverse the 30 degrees inclination. The average current consumed and the volume of sand displacement was small for modified wheel rover compared to conventional wheel rover for each degree of sand surface inclination.

2.8 Conclusion

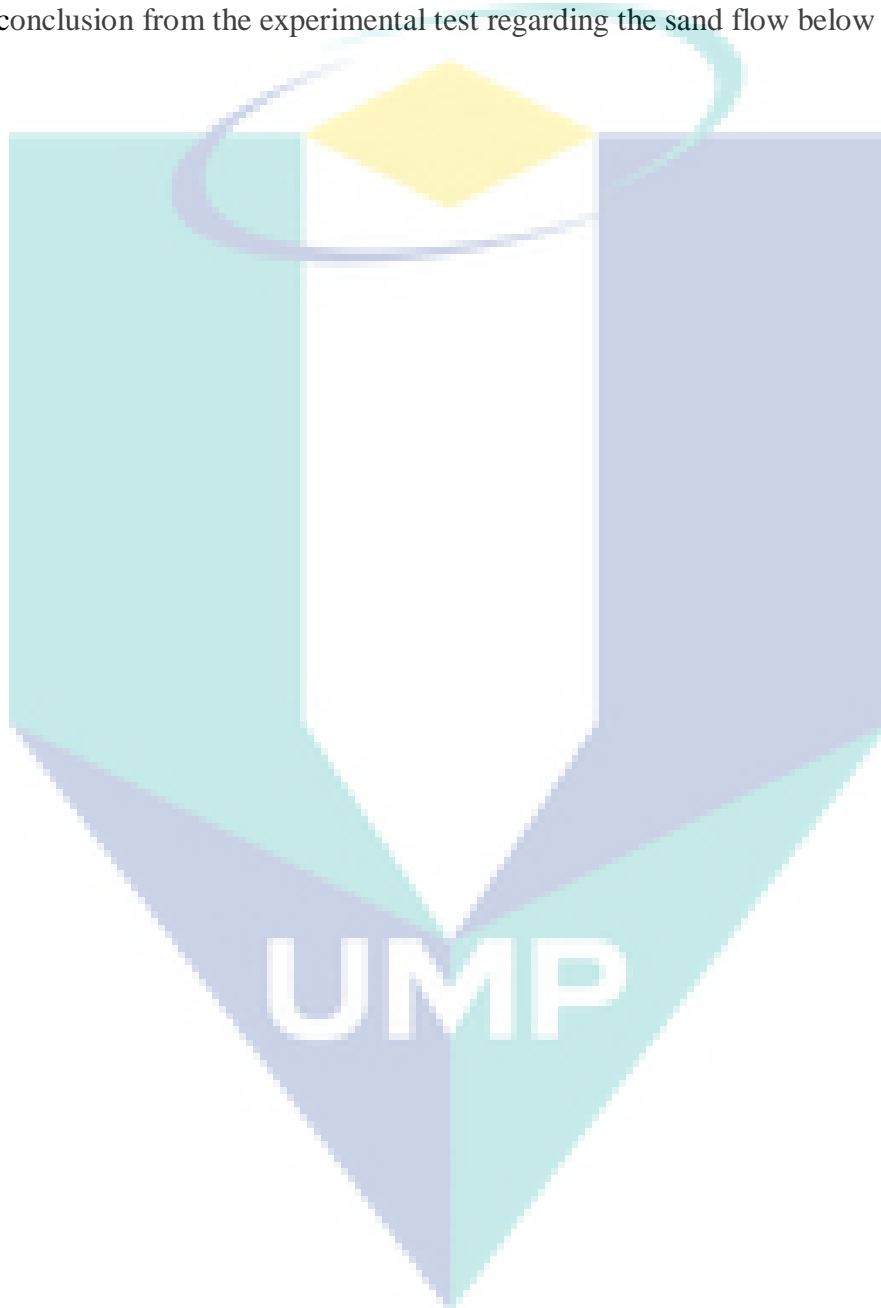
There are many methods for simulation modelling. One example of simulation modelling is terramechanics modelling. Three common methods for terramechanics modelling are Bekker method, dynamic Bekker method and DEM (Discrete Element Method). Terramechanics modelling is a study of soil properties and commonly used to model a simulation design that related with wheeled or tracked vehicles on a various surface. The other simulation modelling method is CFD (Computational Fluid Dynamics). This method commonly related to fluid flow simulation design problem. Next is FEM (Finite Element Method). FEM is useful to design a complicated geometries, loading, and material properties where analytical solutions cannot be obtained. For this research study, DEM will be used in the simulation modelling.

DEM is a numerical approach for computing the motion and effect of a large number of small particles such as granular flows, powder mechanics, and rock mechanics. It has been used in engineering problems such as in granular and discontinuous materials. DEM is one of the methods used for terramechanics model. Previously, researchers used DEM for their research simulation. For example, Nakashima, H., et al. used DEM to analyze the performance of a lugged wheel for a lunar micro rover on slope terrain [7]. Besides that, Nakashima, H. and T. Kobayashi also used DEM simulation to investigate the effect of gravity on rigid wheel sinkage, motion resistance, and slip [18].

Ibrahim, A.N., et al. (referred case study) purposed a prototype that can be used as a solution to solve the problem of wheel rover that tends to stuck into an unconsolidated sandy incline. He purposed a new prototype design of wheel rover that attached with “assistive grousers” [3]. The assistive grousers used to minimize sand movement and subsequent sinkage. The experiment was run and the result for conventional wheel rover (wheel that attached with fixed grousers) and modified wheel rover (wheel that attached with assistive grousers) was recorded. At the end of the experiment, the data that was recorded shows modified wheel rover perform more efficient compared to conventional wheel rover as discuss in **section 2.6.3** and **2.6.4**.

So in this research study, a simulation modelling will be carried out based on the experimental test that has been done by Ibrahim, A.N., et al. 2D simulation modelling by using DEM will be used to observe the interaction between the grousers and sand. By the

simulation modelling, the parameter such as sand flow below the rotating wheel can be observed. 2D circular shape particles (represent as sand flow) will be designed. 2D model was chosen instead of 3D model in order to minimize computation time and maximizing the number of DEM elements used. The result from the simulation modelling will be validated by the experimental result. And the observation from the simulation modelling will verify the hypothesis conclusion from the experimental test regarding the sand flow below the wheel.



CHAPTER 3

RESEARCH METHODOLOGY

3.1 Introduction

In this chapter, the methodology details for the research study are presented. The research methodology for this research study was divided into two subtopics; research methodology process and research component. In research methodology process subtopic, it will discuss briefly the overview of the actions or steps for developing the research model. And the research component shows the supporting components for the development of research model. This chapter will also discuss the DEM simulation as well as the simulation preparations.

3.2 Research Methodology Process

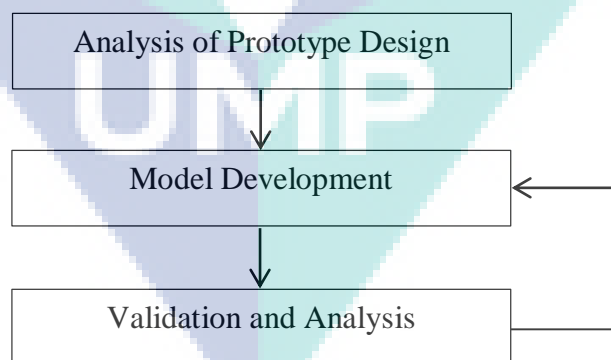


Figure 3.1: Research Methodology Process

As shown in Figure 3.1 the research methodology process was divided into a few parts. Each part has its own purpose, process, and output as below:

i. Analysis of Prototype Design

Purpose	- Deep understanding of the previous hardware experiment conducted by Ibrahim, A.N., et al. in order to know the prototype design and the performance of wheel rover.
Process	- Review the prototype design and how the experiment was conducted. The experiment was conducted by using two type of wheel rover which is conventional wheel rover and modified wheel rover (assistive grousers). Both wheel rovers were tested to climb sand surface inclination slope at different angles inclination. The result from both wheeled rovers was compared.
Output	- The experimental result from the previous study was obtained. From the result, modified wheel rover (with assistive grousers) more effective compared to conventional wheel rover (without assistive grousers).

ii. Model Development

Purpose	- Studying the concept of Discrete Element Method (DEM) that will be used in the simulation modelling. A simulation modelling will be carried out based on the prototype of wheel rover from the experimental test in order to analyze the sand-grouser interaction.
Process	- A simulation modelling test will be carried out based on the prototype model of wheel rover (conventional and modified wheel rover) from the previous study. 2D conventional wheel rover and modified wheel rover will be model by using SOLIDWORKS software. DEM will be used as the simulation method.
Output	- The simulation modelling will show the interaction between grouser and sand. The simulation result will explain why modified wheel rover more effective compared to conventional wheel rover and how the modified wheel rover solves the sunken wheel problem.

3.3 Research Component

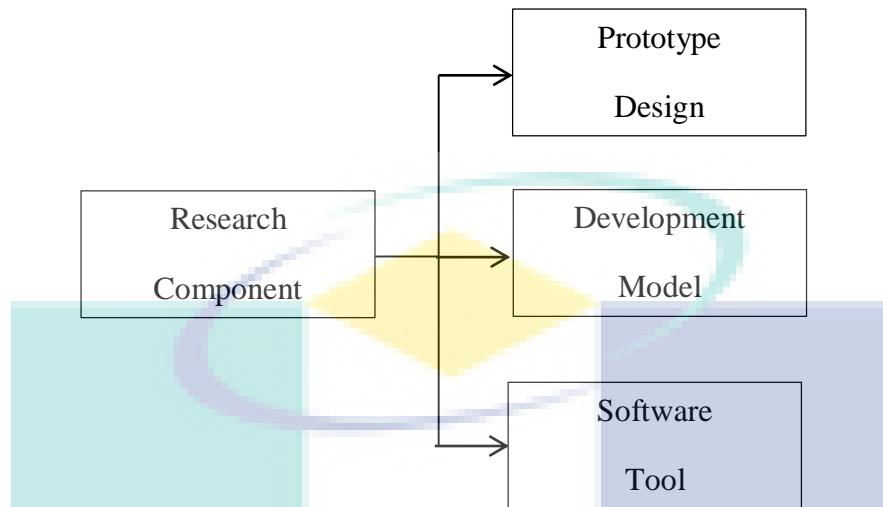


Figure 3.2: Research Component

Figure 3.2 above shows the main component of this research study in order to achieve the objectives of this study. The prototype design refers to the previous experiment model that was conducted by Ibrahim, A.N., et al. The development model is the simulation modelling design process that will be conducted in this research study. And the software tool is the software that will be used for the simulation process which is DEM software.

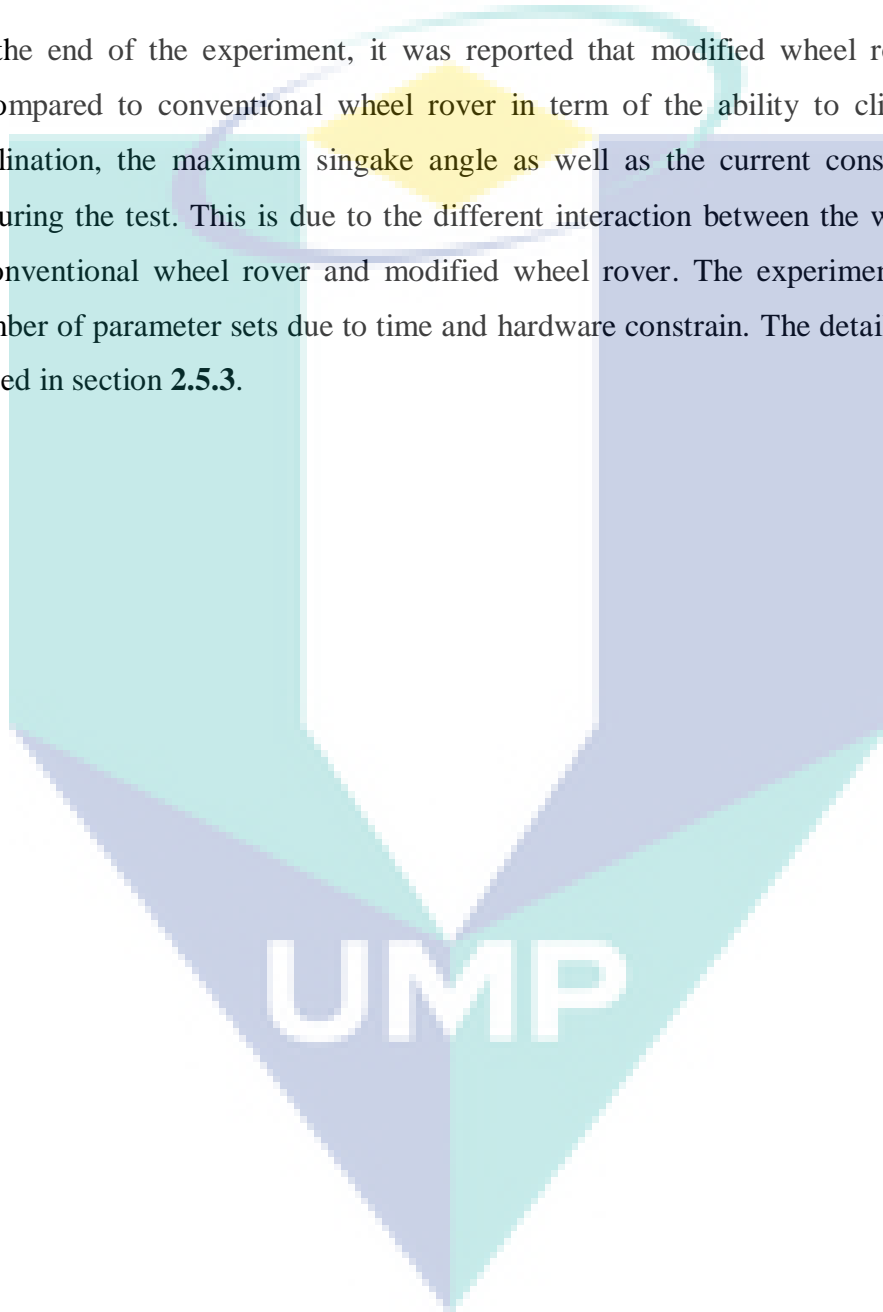
3.3.1 Prototype Design

Today, wheeled rover becomes the focus of study by researchers in order to improve the mobility performance of robot especially in an unconsolidated sand incline. When traverse in an unconsolidated sandy incline, lightweight wheeled rover have a high risk to get stuck in the unconsolidated sandy incline as the wheels tend to sink into the sand. The example of an improvement that has been made by the previous researcher to overcome this problem has been reported in [7] where Nakashima, H., et al. increased the height and number of grousers that attached to the wheel. So it increased the gross traction and running resistance during slope locomotion.

The prototype design for this research study is based on Ibrahim, A.N., et al. experimental test. Ibrahim, A.N., et al. purposed a new prototype design by using “assistive grousers” that attached to the wheel in order to minimize the sand movement and subsequent

sinkage [3]. In the experiment, two types of wheeled rover were used which is conventional wheel rover (attached with fixed grouser) and modified wheel rover (attached with assistive grouser). Both wheeled rovers were tested an indoor sand incline mobility test field by using Toyoura sand and it was tested at different angles of inclination with different grouser's length (Table 2.2).

At the end of the experiment, it was reported that modified wheel rover is more effective compared to conventional wheel rover in term of the ability to climb the sand surface inclination, the maximum singake angle as well as the current consumption that produced during the test. This is due to the different interaction between the wheel and the sand for conventional wheel rover and modified wheel rover. The experimental test used limited number of parameter sets due to time and hardware constrain. The detail of the result was discussed in section **2.5.3**.



3.3.2 Development Model

Development model refers to the simulation design to investigate the interaction between grouser and sand. The flow chart below shows the process of the simulation.

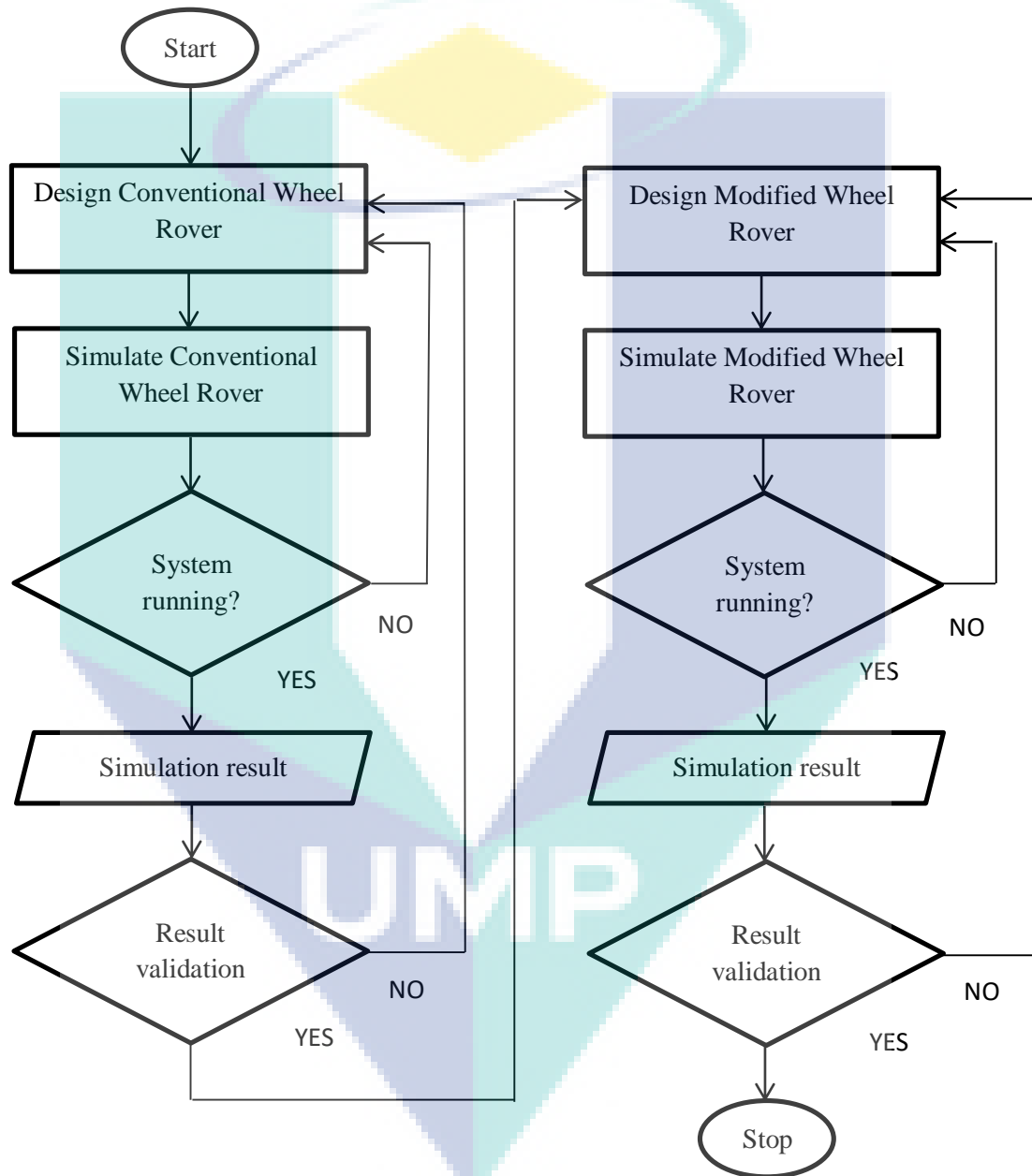


Figure 3.3: Simulation Process Flow Chart

Figure 3.3 shows the process flow of the simulation. This development model (simulation design) was built in order to observe the interaction between the wheel and the sand because based on the experiment alone it cannot verify how modified wheel rover become more effective compared to conventional wheel rover. From this simulation design, the parameters such as sand flow below the rotating wheel can be observed through the simulation modelling.

For the simulation modelling, conventional wheel rover and modified will rover will be designed by using SOLIDWORKS software and then imported to DEM software. By using the DEM software the wheel rover will be simulated with the sand particles. The motion of discrete solids or particles is obtained by DEM which applies Newton's law of motion to every particle.

After the design phase is completed, the wheel system model will be tested. The interaction between each wheel and particle (sand) will be observed and the result will be validated by the experimental result. The interaction result from both models will verify the hypothesis conclusion of experimental result regarding the sand flow during the wheel is rotating.

3.3.3 Software Tool

The software that will be used for the simulation modelling is DEM software. It is used to model/design and analyze bulk materials such as coal, mined ores, soil, tablet and powders. By using the software it will shows how bulk materials interact with the object. As for this study, the interaction between the sand and the wheel rover can be observe.

3.4 DEM Simulation

Discrete Element Method (DEM) that was initially purposed by Cundall as a computational tool for analyzing the wheel-sand interaction in terramechanics. DEM is a method to model granular materials such as sand, soil, rock or dust as a collection of individual particles which generate forces and torques upon contact with other elements. By using DEM, researchers can perform studies which are difficult to conduct experimentally.

For example, examining the influence of gravitation force on motion resistance [18]. In DEM simulation, the shape of the particle influences the accuracy of the simulation results. For this research study, 2D circle particle will be used.

The advantage of 2D circle is they require significantly less computational time and unable to interlock, while free to rotate in place without disturbing other sand particles. The force acting between two particles and between one particle and a wall consist of the sum of two vector forces which are Hertzian style friction forces F_{Hertz} [29-31] and cohesive force $F_{cohesion}$ [32]. The Hertzian contact force-displacement relationship varies non-linearly with contact area and is the sum of normal and tangential forces. Forces normal to the contact plane (along the unit vector between particles) as below

$$F_{Hertz,n} = \sqrt{\delta \frac{R_i R_j}{R_i + R_j}} (k_n \delta n_{ij} - m_{eff} \gamma_n v_n) \quad \text{Eq 3.1}$$

δ = Overlap length of two particles

$R_{i/j}$ = Radius of each particle

k_n = Normal elastic spring constant

n_{ij} = Unit vector connecting the center of each particle

γ_n = Normal viscoelastic damping constant

v_n = Normal component of the relative velocity of the two particles

m_{eff} = Effective mass of two particles of mass $M_{i/j}$

$$m_{eff} = \frac{M_i M_j}{M_i + M_j} \quad \text{Eq 3.2}$$

Figure 3.4 below show the contact model for particle-particle force/torque interactions [33]

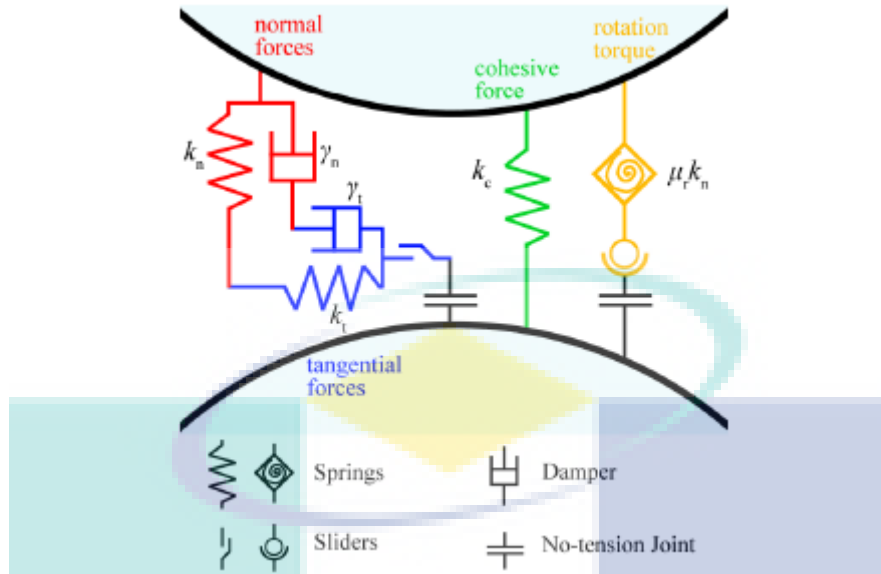


Figure 3.4: DEM contact model for particle-particle force/torque interactions

The equation for forces tangential to the contact plane as below

$$F_{Hertz,t} = \sqrt{\delta \frac{R_i R_j}{R_i + R_j}} (k_t \Delta s_t + m_{eff} \gamma_t v_t) \quad \text{Eq 3.3}$$

- k_t = Tangential elastic spring constant
- Δs_t = Tangential displacement vector between the two particles for their entire contact duration
- γ_t = Tangential viscoelastic damping constant
- v_t = Tangential component of the relative velocity of the two particles

An upper limit exists for tangential forces through the Coulomb criterion given as below

$$\text{if } |F_t| > \mu_c |F_n| \text{ then } |F_t| = \mu_c |F_n| \quad \text{Eq 3.4}$$

- μ_c = Static yield coefficient

To provide cohesive forces between particles, a simplified Johnson-Kendall-Roberts model [9] will be used. While two particles are in contact, an additional normal forces act to maintain particle contact as given below

$$F_{cohesion} = -k_c A n_{ij} \quad \text{Eq 3.5}$$

$$\text{where } A = -\frac{\pi}{4} \cdot \frac{(d_{ij} - R_i - R_j) \cdot (d_{ij} + R_i - R_j) \cdot (d_{ij} - R_i + R_j) \cdot (d_{ij} + R_i + R_j)}{d_{ij}^2}$$

k_c = Cohesion energy density (units J/m³)

A = Contact area of the two particles

d_{ij} = Distance between the center of two particles

In this research study, circle particles will be used with finite mass. Particles are able to rotate given an applied torque, either as a result of the previous mentioned forces or as a result of rolling friction. Using a constant directional torque model [34], a torque contribution T_{rolling} can result from the relative angular velocity between two particles, given by

$$T_{\text{rolling}} = \text{proj}_{t_{ij}} \left(\mu_r k_n \frac{R_i R_j}{R_i + R_j} \frac{\omega_i - \omega_j}{|\omega_i - \omega_j|} \right) \quad \text{Eq 3.6}$$

$\text{proj}_{t_{ij}}$ = Projection into the shear plane

μ_r = Rolling resistance coefficient

$\omega_{i/j}$ = Angular velocity of each particle

3.5 Simulation Preparation for Conventional Wheel Rover and Modified Wheel Rover

Before a simulation can be performed it must be prepared first. Everything in the simulation must be prepared by the researcher, from the simulation space to the initial location of each individual particle. The preparation steps are wheel building and DEM setup.

For the wheel building, two types of wheel will be modelled which are Conventional Wheel Rover and Modified Wheel Rover by using SOLIDWORKS. These two types of rover were used in the experimental test. The parameter for both rovers as listed in Table 3.1. For DEM setup, it involve DEM software where the particles that represent sand will be designed. The wheel design from the SOLIDWORKS will be imported to the DEM software for simulating process. From the simulation, the interaction between the sand and the wheel will be observed. Besides, the parameter that affect the sand movement also will be observed.

Table 3.1: Wheel properties [35]

Parameter	Conventional Wheel Rover	Modified Wheel Rover
Wheel diameter (mm)	296	296
Type of grouser	Fixed grouser	Assistive grouser
Grouser length (mm)	20, 40, 60, and 80	50, 70, and 90
Number of grouser	12	6

3.5.1 Wheel Building

Wheel building part was divided into two set of simulation. First set involved single grouser and second set involved multiple grouser. For the first set of simulation, conventional wheel rover and modified wheel rover with single grouser was designed. The focus is to observe how a single grouser and sand particles interact for one rotation (one pass). The design included the wheel, grouser and sand box. The design parameter were listed in Table 3.2 below. Figure 3.5 (a-b) below show the conventional wheel rover with single grouser for 80 mm grouser length at 0 and 30 degree angle slope. Figure 3.6 (a-b) below show the modified wheel rover with single grouser for 90 mm grouser length at 0 and 30 degree angle slope.

Table 3.2: Design parameter

Parameter		Conventional Wheel Rover	Modified Wheel Rover
Wheel	Diameter (mm)	296	
	Width (mm)	90	
Type of grouser		Fixed grouser	Assistive grouser
Grouser	Length (mm)	80	90
	Width (mm)	90	
	Thickness (mm)	2	
Number of grouser			1
Sand box	Length (mm)	520	
	Height (mm)	220	
	Width (mm)	190	260
Slope angle		0 and 30 degree	

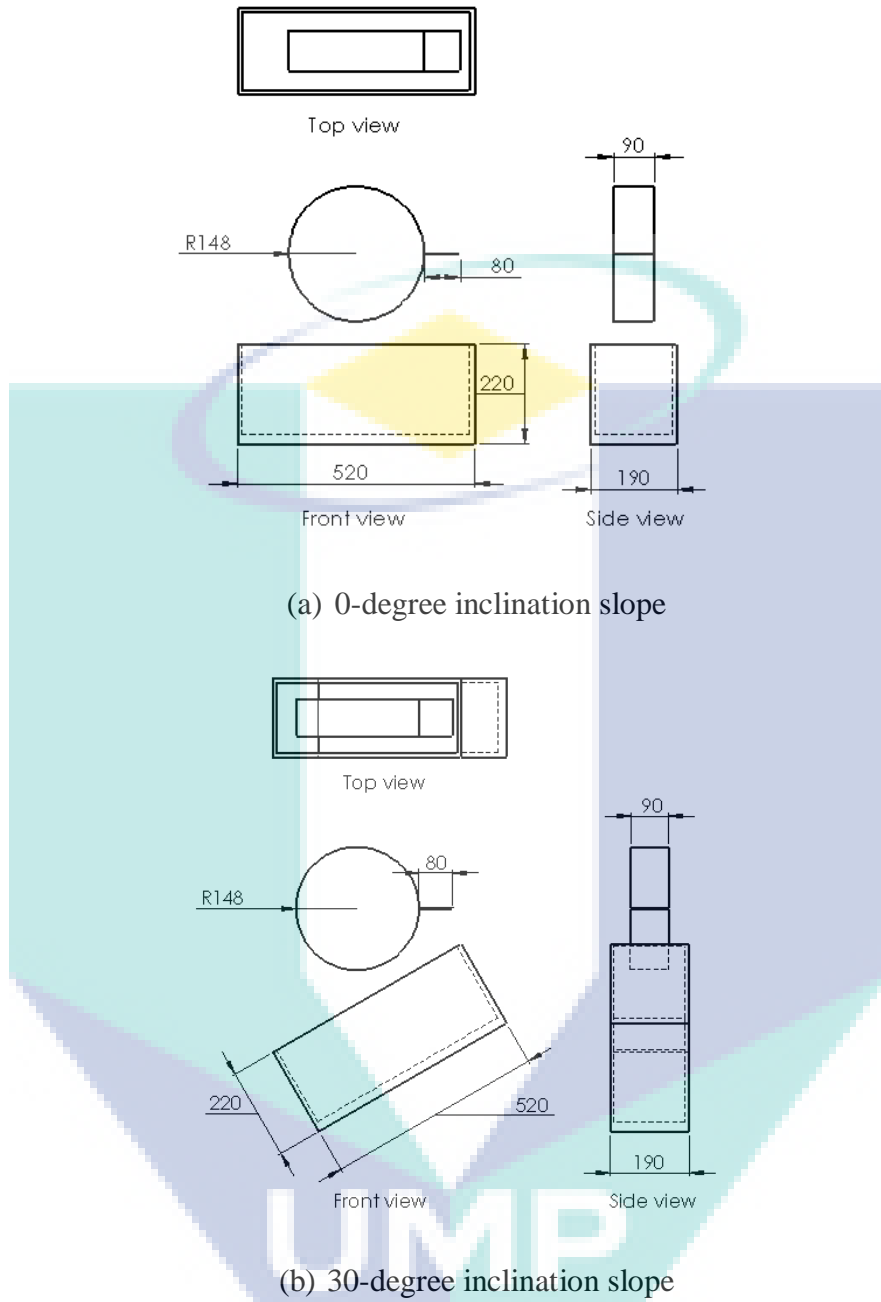


Figure 3.5: Conventional Wheel Rover with single fixed grouser at (a) 0-degree slope and (b) 30-degree slope

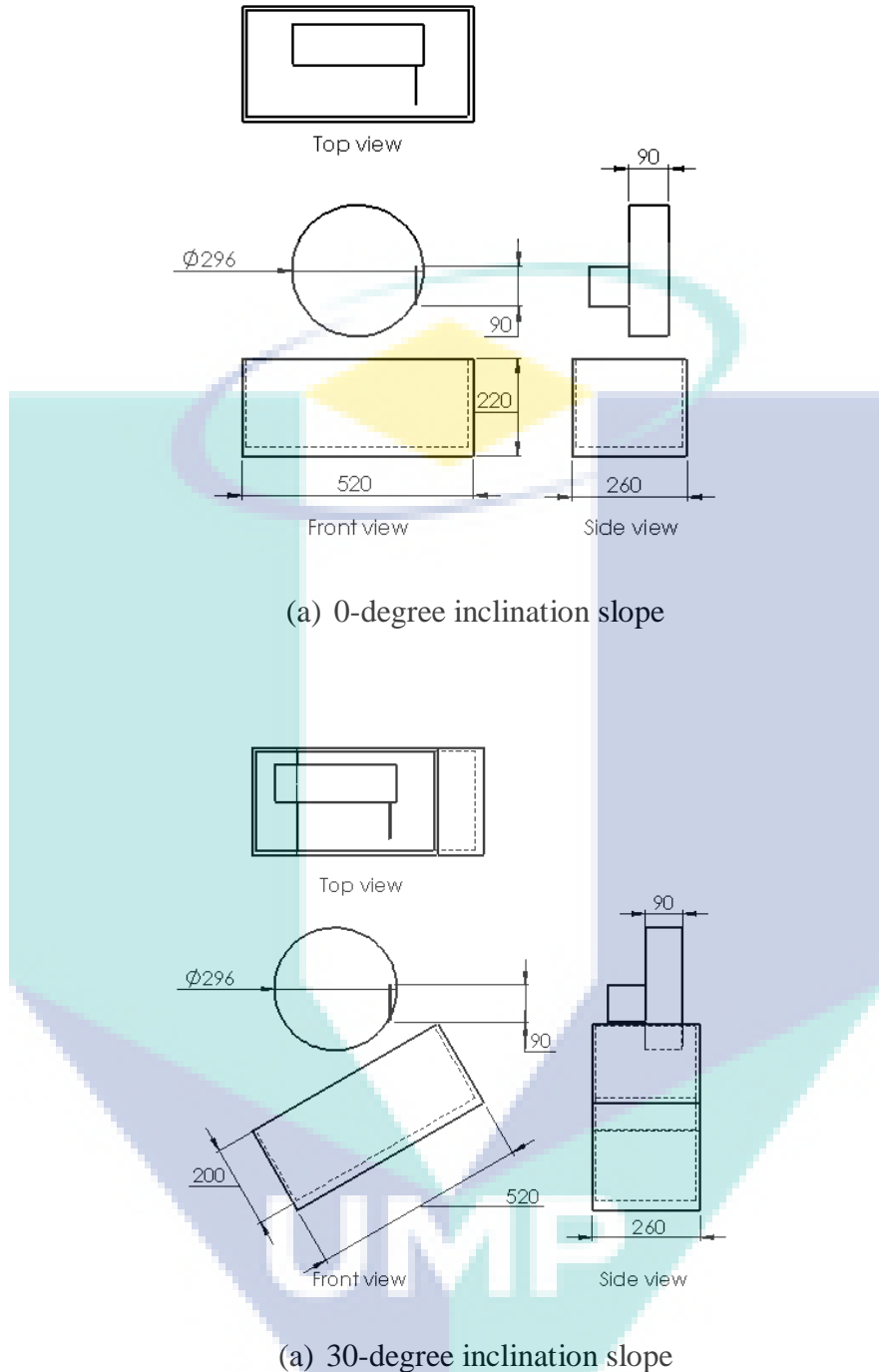


Figure 3.6: Modified Wheel Rover with single assistive grouser at (a) 0-degree slope and (b) 30-degree slope

Figure 3.7 below shows the design of the simulated wheel rovers and 0 and 30 degree angle slope. The blue arrow shows the direction of rotation. The initial position is the point when the grouser starts to enter the sand and the final position when the grouser starts to exit the sand. To assist in the analysis of the result, each recorded data was divided into three parts of grouser angle ranges θ_1 , θ_2 and θ_3 with the values as shown in Table 3.3.

The focus of this set of simulation is on observing the effect of grouser movement on the subsurface particle movement. So the simulation was done with the wheel fixed to a static

position and rotate at constant speed which is 1RPM. This setup will simulate the condition of the wheel rotating under 100% slip condition as the wheel remains static in place while the wheel rotate at a constant speed. By observing the movement of particles under this condition, it can be predicted that the amount of traction that the grouser are able to create as more particles moved by the grouser subsurface motion means that more inter-particle friction could be generated.

Table 3.3: Values of grouser angle range

Grouser	0-degree slope		30-degree slope	
	80 mm	90 mm	80mm	90mm
	fixed	assistive	fixed	assistive
θ_1 (°)	0-45	0-52	0-38	0-46
θ_2 (°)	45-90	52-104	38-76	46-92
θ_3 (°)	90-135	104-156	76-114	92-138

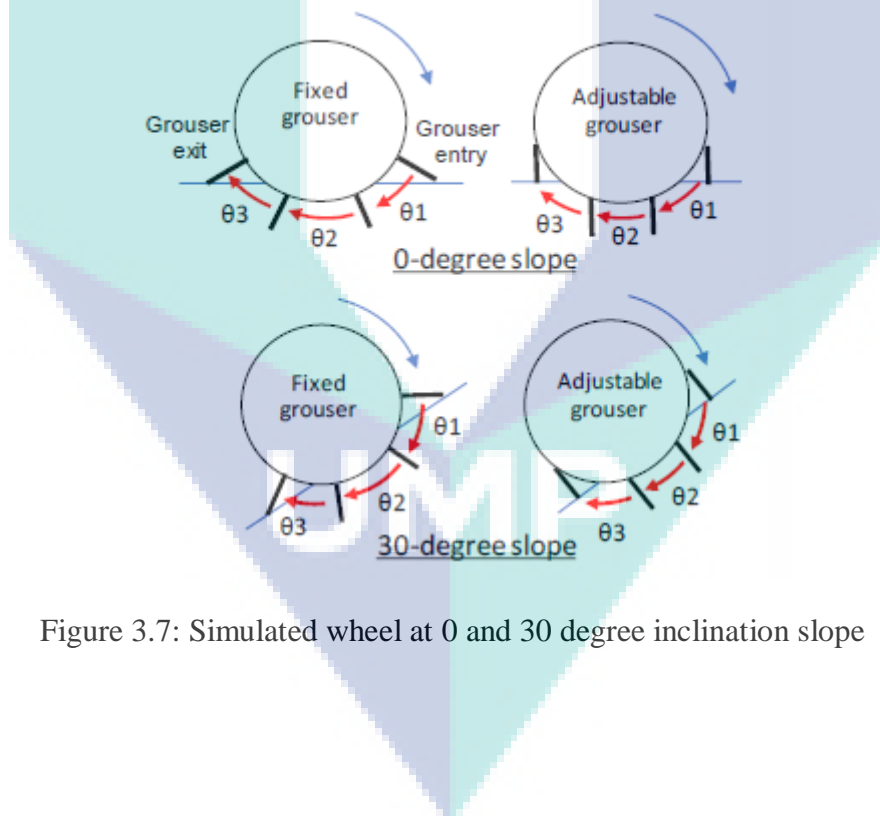


Figure 3.7: Simulated wheel at 0 and 30 degree inclination slope

3.5.2 DEM Setup

One of the method to model the dynamics of solid particles that interact with each other is DEM. For this simulation, DEM was used to model the particles that represent sand. The DEM parameter as listed in Table 3.4 below. The particles (sand) was modelled to fill the sand box. The simulation will involve the interaction between the wheel and the particles.

Table 3.4: DEM parameter

Parameter	Value
Radius of each particles, r (mm)	5
Density of particle (kg/m^3)	2678
Gravity	9.81

3.6 Simulation Preparation for Assistive Grouser Movement Model

The next step to continue this study is to design a model for assistive grouser that will be attached to the wheel rover. This simulation focus on one single grouser that move horizontally (translational) similar to assistive grouser movement pattern in the previous set. Figure 3.8 below shows the assistive grouser model that was simulated at level inclination slope (0-degree inclination slope) and Table 3.5 shows the parameter of the model. For this simulation set, the size of particle used is radius 3 mm. The size used was smaller compared to the previous set in order to make it more similar to the real particle size.

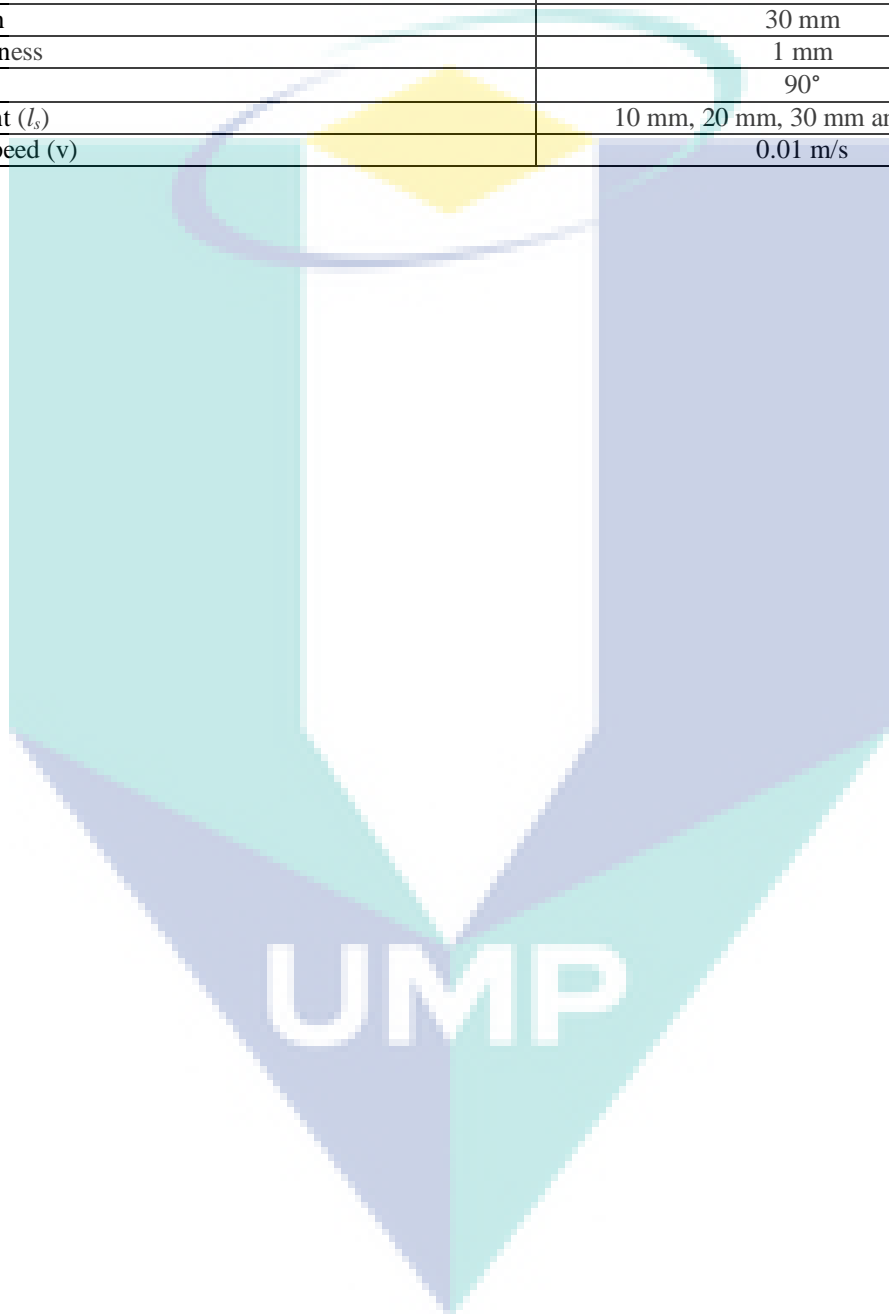


Figure 3.8: Assistive grouser model

Figure 3.8 shows the model of assistive grouser with a single grouser. The reason why the focus is on single grouser is to make the observation move easily to observe and to understand. The initial position is where the grouser start to move and the final position is where the grouser stop moving. The red arrow shows the direction of grouser movement and the gray area is the traveled area phase, α is the angle between the grouser and the sand surface. Next, l_s is the sinkage height when the grouser enter the sand surface, and “A” is the destructive area where the particle moved/accumulated by the grouser movement. The translation speed (v) for every sinkage length are same.

Table 3.5: Assistive grouser model parameter

Parameter	Value
Grouser length	110 mm
Grouser width	30 mm
Grouser thickness	1 mm
α	90°
Sinkage height (l_s)	10 mm, 20 mm, 30 mm and 40 mm
Translation speed (v)	0.01 m/s



CHAPTER 4

RESULT AND DISCUSSION

4.1 Introduction

In this chapter, the result from the simulation will be show and discuss. The result will covered the particle velocity pattern and average particle displacement for conventional wheel rover and modified wheel rover with single grouser at one rotation (one pass). Table 4.1 below shows the particle velocity pattern when the grouser start to rotate. Figure 1 and 2 shows the average sand displacement graph. Next is the simulation result from assistive grouser model.

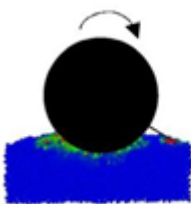
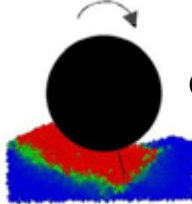
4.2 Performance Evaluation for Conventional Rover and Modified Rover

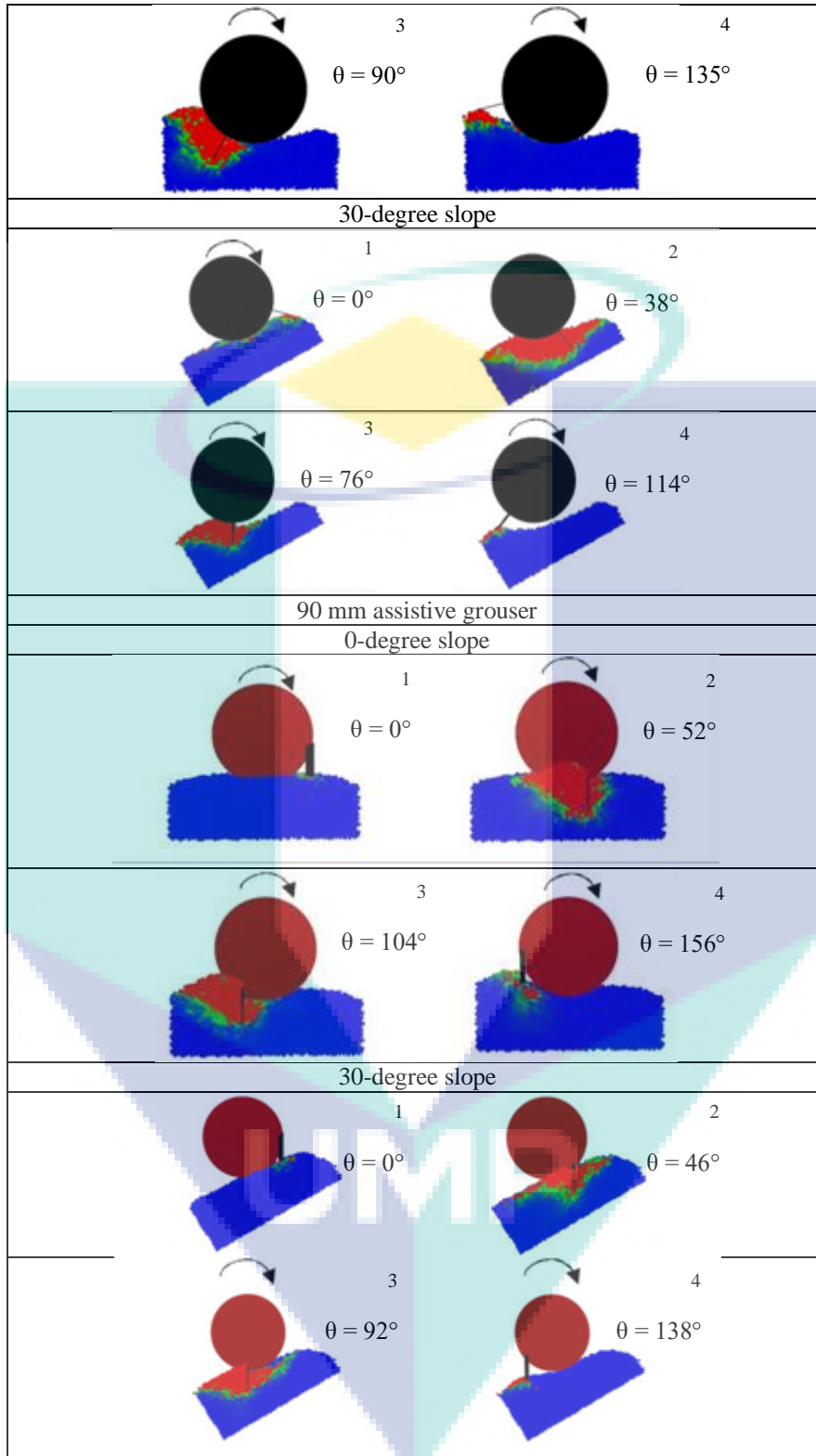
The performance evaluation criterion will be explained below.

4.2.1 Particle Velocity Pattern

Table 4.1 below shows the result from the simulation of wheel rotation for 80 mm fixed grouser and 90 mm assistive grouser at 0 degree angle slope and 30 degree angle slope. It shows the velocity magnitude of the particles when the wheel rotates.

Table 4.1: Particle velocity distribution

80 mm fixed grouse	
0 degree slope	
	1 $\theta = 0^\circ$
	2 $\theta = 45^\circ$



The blue color represents minimum velocity which is $1.75E-003$ m/s. The green color represents the middle velocity which is $6.75E-003$ m/s. The red color represents maximum velocity which is $8.18E-003$ m/s.

From the result, we can observe the movement of particles as the grouser of the wheel moves under the sand surface. At 0-degree slope the animation shows that the fixed grouser displaced a wider area of sand particles until the back of the wheel compared to assistive

grouser for the first one-third of the wheel rotation. It can be confirmed by counting the actual number of particles that moves during the wheel rotation simulation. For grouser angle range θ_1 , 80 mm fixed grouser moved 13511 particles compared to 90 mm assistive grouser with 12975 particles. The rotating movement of the fixed grouser was affecting the particles positioned at the backside of the wheel even at the beginning of the rotation. In a high slip condition, this could be contributing to a high sinkage for the wheel, as the soft sand are displaced from under the wheel toward the back of the wheel, as the wheel digs into the surface.

For grouser angel range θ_2 , the difference of the spread of the particles displaced by the grouser movements and be observe. Fixed grouser only effects the particles in the way of its rotation, which is from under towards the surface. This movement mainly contributes towards the digging of the wheel for a fixed grouser wheel. For assistive grouser, it effects the particles until further away to the back of the wheel, which is because the almost translational movement of the grouser is pushing the grouser in the X direction instead of Y direction that can cause digging by the wheel. Fixed grouser 80 mm moved 12813 particles while assistive grouser 90 mm move 14162 particles.

For grouser angle range θ_3 , fixed grouser 80 mm still moving the sand as the grouser exits the sand surface. While the assistive grouser have a cleaner uninterrupted exit from the sand subsurface.

At 30-degree slope, the result similar to 0-degree slope. For the one third of rotation, angle range θ_1 , fixed grouser displaced a wider area of particles extended to the particles behind the wheel compared to assistive grouser. At grouser angle θ_1 , fixed grouser 80 mm moved 13692 particles while assistive grouser moved 12527 particles.

For grouser angle range θ_2 , it show a similar pattern for particles displaced for both fixed and assistive grouser. This could be caused by the tendency for the particles to flow to the backside of the wheel on the slope, and because of the angle of the assistive grouser tested which is 0 degree relative to the vertical axis. A different result may be obtained if a different grouser angle was tested by using assistive grouser. The number of particles moved for 80 mm fixed grouser was 13032 and 14331 for assistive grouser. Lastly, after the grouser exit the sand surface, a large amount of sand was displaced from under the wheel for fixed grouser compared to assistive grouser.

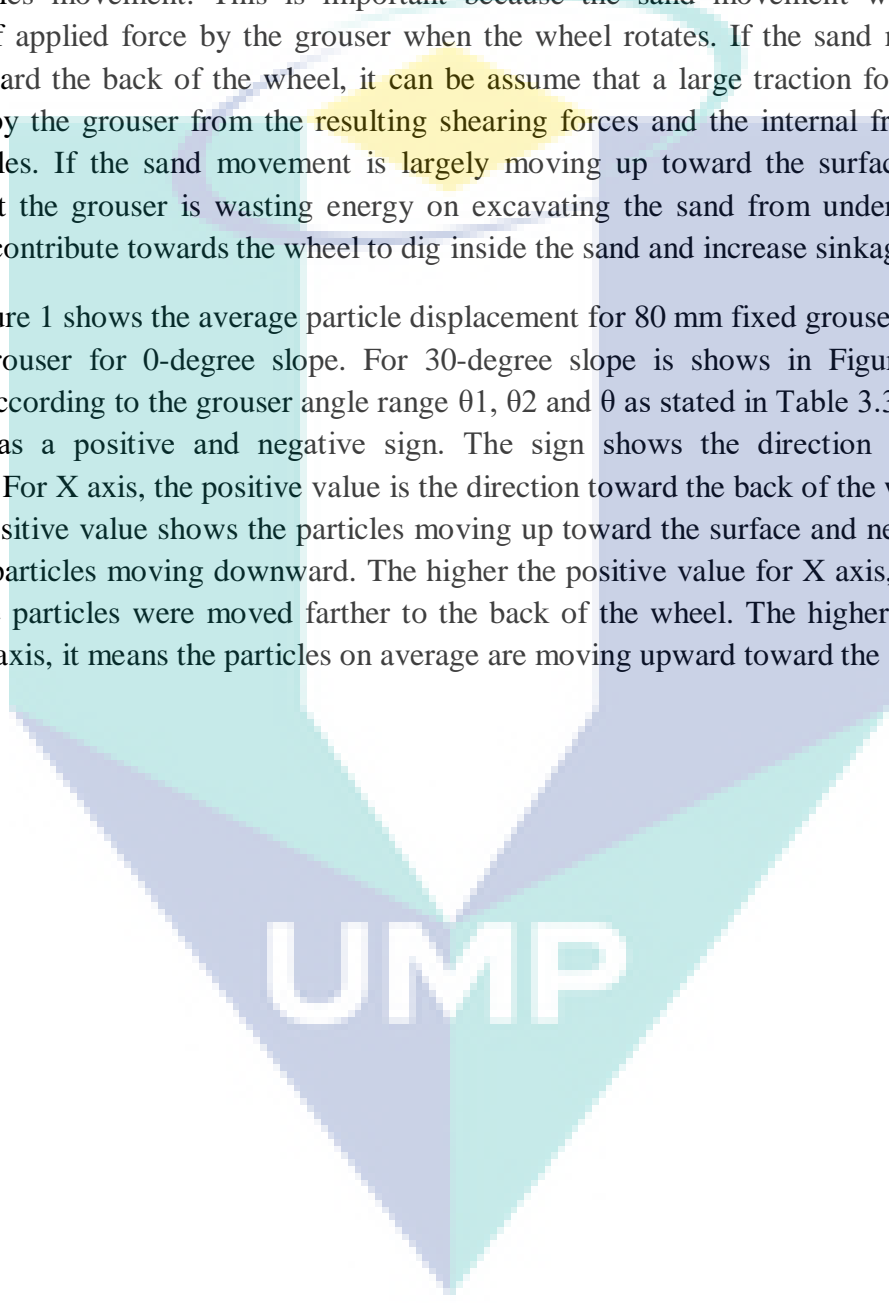
At the beginning of the wheel rotation, the rotation movement of the fixed grouser will affect a large area of sand particles extending until the back of the wheel, while reduce area when on 0-degree slope. However the assistive grouser maintain an almost similar area of effect throughout the grouser movement on 0-degree slope. On 30-degree slope, fixed grouser displaced a large number of particles from under the wheel compared to assistive grouser. A same pattern can be seen for the affected area of sand particles. This could be caused by the chosen angle for the assistive grouser in this set of simulation. From this result, it shows that if the wheel experiencing slipping on a steep slope of soft sand surface, a long-

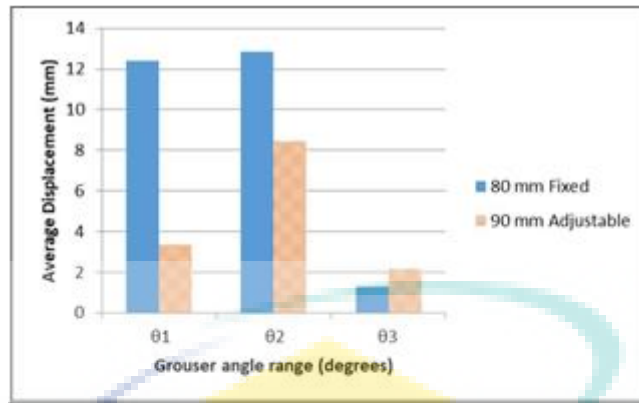
fixed grouser might cause more sand particles to be displaced from under the wheel to the back of the wheel and can cause the wheel sink inside the sand.

4.2.2 Average Particle Displacement

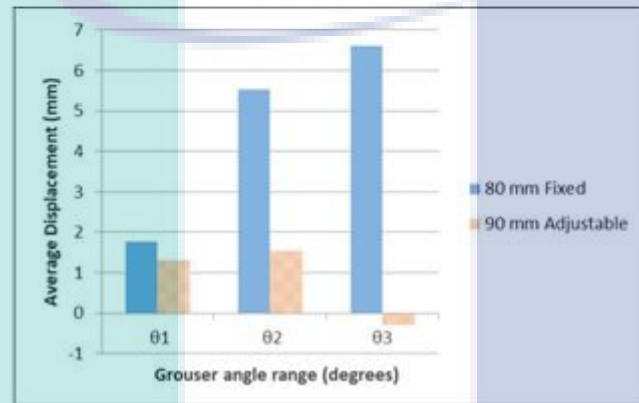
The value of particle displacement distance could help in understanding the pattern of sand particles movement. This is important because the sand movement will show the direction of applied force by the grouser when the wheel rotates. If the sand movement is largely toward the back of the wheel, it can be assume that a large traction force could be generated by the grouser from the resulting shearing forces and the internal friction of the sand particles. If the sand movement is largely moving up toward the surface, it can be assume that the grouser is wasting energy on excavating the sand from under the surface which can contribute towards the wheel to dig inside the sand and increase sinkage.

Figure 1 shows the average particle displacement for 80 mm fixed grouser and 90 mm assistive grouser for 0-degree slope. For 30-degree slope is shows in Figure 2. It was separated according to the grouser angle range θ_1 , θ_2 and θ as stated in Table 3.3. The values recorded has a positive and negative sign. The sign shows the direction of particle's movement. For X axis, the positive value is the direction toward the back of the wheel. For Y axis, the positive value shows the particles moving up toward the surface and negative value shows the particles moving downward. The higher the positive value for X axis, it means on average the particles were moved farther to the back of the wheel. The higher the positive value of Y axis, it means the particles on average are moving upward toward the surface.





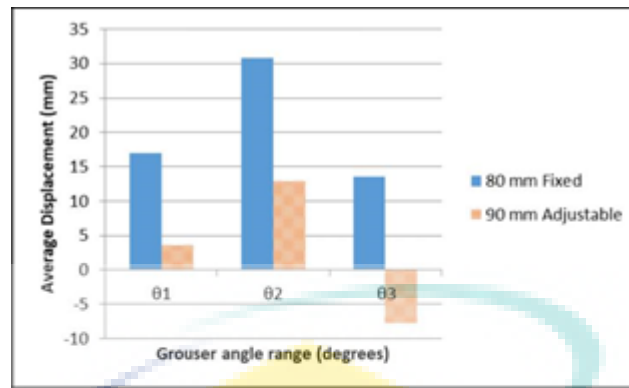
(a) X axis direction



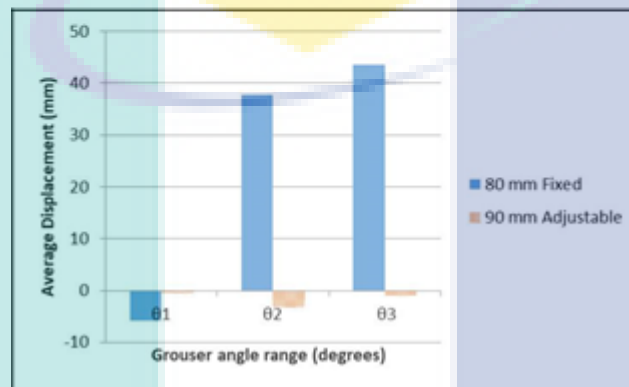
(b) Y-axis direction

Figure 1: Average sand displacement at 0-degree inclination slope for X-axis direction (a) and Y-axis direction (b)

UMP



(d) X axis direction



(c) Y-axis direction

Figure 2: Average sand displacement at 30-degree inclination slope for X-axis direction (a) and Y-axis direction (b)

Figure 1 show the average particle displacement graph that move at X-axis and Y-axis for both grousers type at 0-degree slope. For X-axis, at 0-degree slope the fixed grouser generated a higher amount of displacement for grouser angle range θ_1 and θ_2 . As the 80 mm fixed grouser is quite long, it able to move a large amount of particles to a longer distances while the assistive grouser only able to move particles in a limited range because it maintaining a constant angle at the sand subsurface. For θ_3 , the adjustable grouser generated a higher displacement. This is because the fixed grouser is largely moving the particles on Y-axis at the end of the rotation. On the other hand, the assistive grouser still maintaining its angle of movement.

For Y-axis at 0-degree slope, fixed grouser move a large amount of particles upwards toward the surface compared to assistive grouser. The negative sign at θ_3 for assistive grouser means that most of the particles moves downward opposite to the surface. From the graph, fixed grouser shows an increasing pattern of particles that move toward the surface as the wheel continue to rotate. It is not desirable as it shows that the particles are being excavated from under the wheel towards the back of the wheel. This will cause an increasing sinkage as the wheel moves on a sand surface with high slip ratio and might cause the wheel stuck inside the sand. However the assistive grouser generated a relative small displacement in Y-axis due

to the chosen angle of the grouser. It is beneficial for the wheel to generate a large value of negative Y-axis displacement as this will result in a large net force upwards and prevent the wheel from sinking into the sand surface.

Figure 2 shows the average sand displacement at X-axis and Y-axis for both type of grouser at 30-degree slope. At X-axis, the higher displacement generated at θ_2 by fixed grouser where the grouser motion is mostly horizontal. Generally, from the graph, fixed grouser generates bigger displacement compared to assistive grouser for the same reason as when on 0-degree slope. The assistive grouser generated a negative direction displacement at θ_3 due to several particles rolling on its own at the opposite direction at the end of rotation as the exit of the grouser is too smooth for causing displacement in the positive direction.

For Y-axis at 0-degree slope, assistive grouser generate a relatively small displacement. This is caused by the angle of the grouser which is 0-degree to the vertical. When the wheel is rotate, the grouser maintain the angle, which is only generate horizontal displacement. Similar to 0-degree slope, fixed grouser generated large positive Y-axis displacement at the last part of wheel rotation. It means that the particles are being excavated from under the wheel. The negative value at θ_1 fixed grouser means that the grouser is pushing the particles down at the beginning of the rotation as the grouser motion is moving downward.

From the result, it can be seen that the relatively long 80 mm fixed grouser will generate a large displacement of the particles due to the large motion range of the grouser. This large movement will also displace the sand from under the wheel toward the surface which can cause the wheel to sink into the sand, and risking the wheel to get stuck inside the sand surface. For the assistive grouser, setting the grouser angle to be 0-degree to the vertical will generate a small amount of displacement of the particles on Y-axis. If the grouser angle is increase, it could generate a large negative direction of particle displacement which will assist the wheel to reduce the amount of sinkage in soft surface. Besides that, it can be understand that by using a long fixed grouser might generated large forward traction but in condition with slipping it might also contribute toward the wheel getting stuck in the sand.

4.3 Performance Evaluation for Assistive Grouser Model

To continue this study, a simulation for assistive grouser model was designed and simulated. The simulation preparation for assistive grouser model has been discussed in 3.6. The interest of studying and proposing this model of assistive grouser is to observe how sinkage height affect the normal force of the grouser surface and the pattern of destructive area (“A” in figure 3.8).

4.3.1 Normal Force of Grouser Surface

The normal force of grouser surface is where the force was generated when the single assistive grouser start to move from its initial point until it stop (translational motion). The normal force result was compared between the result from equation model and simulation model. For the equation model, least square method was used as below. Based on characteristics of the normal force, an exponential function was chosen to approximate the relationship between horizontal displacement Δx and normal force F_n .

$$F_n = F_o + A e^{-B\Delta x} \quad \text{Eq 3.7 [36]}$$

Where,

F_o = Normal force at steady state

A = Difference between the initial ($\Delta x = 0$) and steady value ($\Delta x = \infty$)

$1/B$ = Displacement constant that denotes the traveling distance of the grouser until arriving at steady state.

Figure 3 below shows the graph from the equation model, Figure 4 shows the graph from simulation model and Figure 5 shows the comparison graph between equation and simulation. The plotted graph is based on a single grouser movement at different sinkage height which is 10 mm, 20 mm, 30 mm and 40 mm.

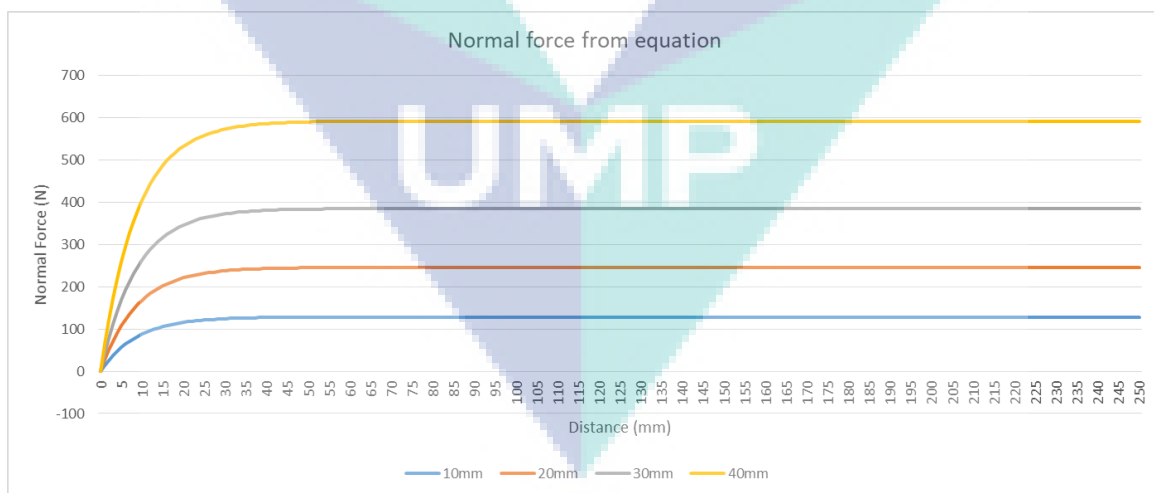


Figure 3: Surface normal force from equation model

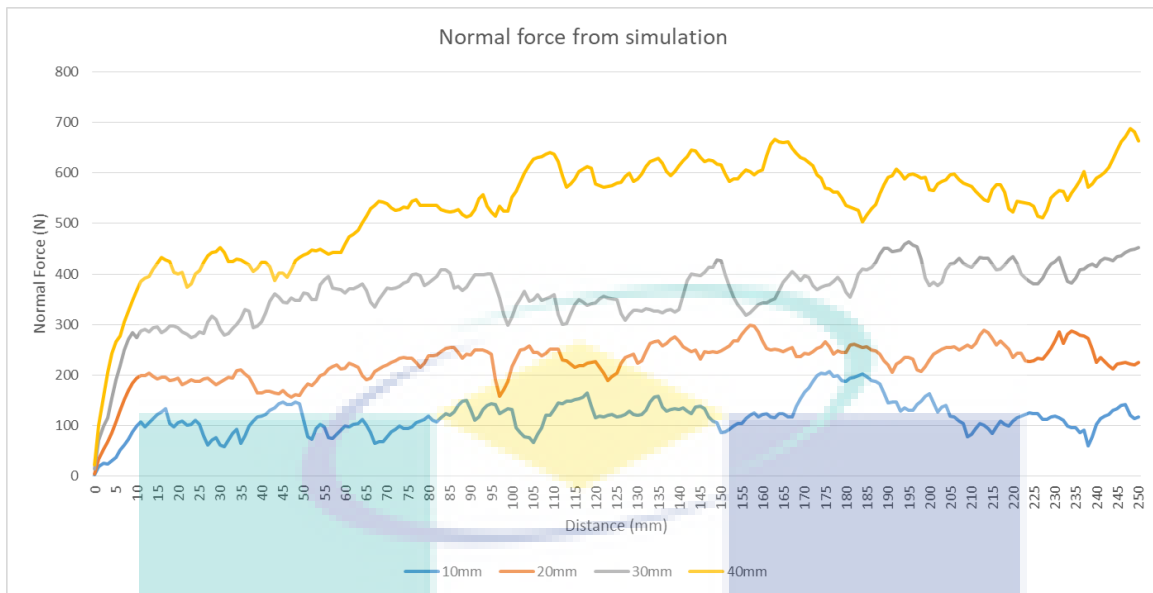


Figure 4: Surface normal force from simulation model

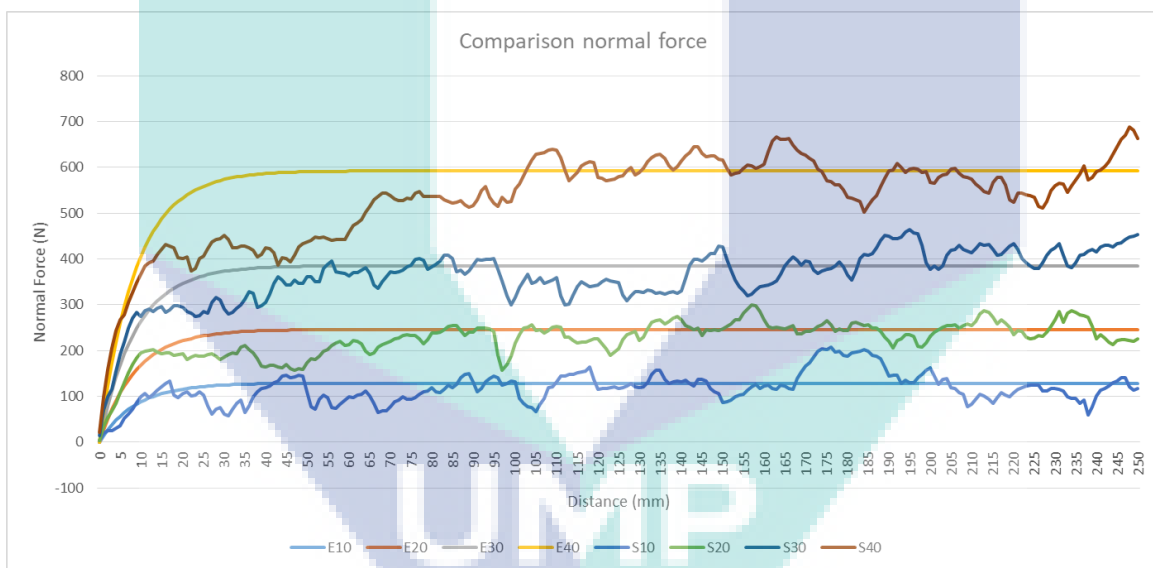


Figure 5: Comparison surface normal force from equation and simulation

Figure 3 shows normal force for grouser surface by using equation model while by using simulation model as in Figure 4. For both graph, blue line represent normal force at 10 mm sinkage height when the grouser move. On the other hand, orange line represent normal force 20 mm sinkage height, gray line represent normal force at 30 mm sinkage height and yellow line represent normal force at 40 mm sinkage height. By observing both graph in Figure 3 and 4, it was noticed that the higher the sinkage height, the higher the normal force generated when the grouser start moving. The pattern from both equation and simulation are same as plotted in Figure 5 for comparison. From the figure, the simulation result shows a little not consistence force during the grouser movement compared to the equation but the pattern of force is still same. The reason why in simulation the result shows is not as smooth

as equation is because of the particle's size. The size of particles used to simulate this assistive grouser model is radius 3 which is double the real size of particle. The bigger size was used compared to the real size in order to reduce the running time and data space memory. The particle size may affect the consistency of the normal force when the grouser moving but still have the same pattern as the model.

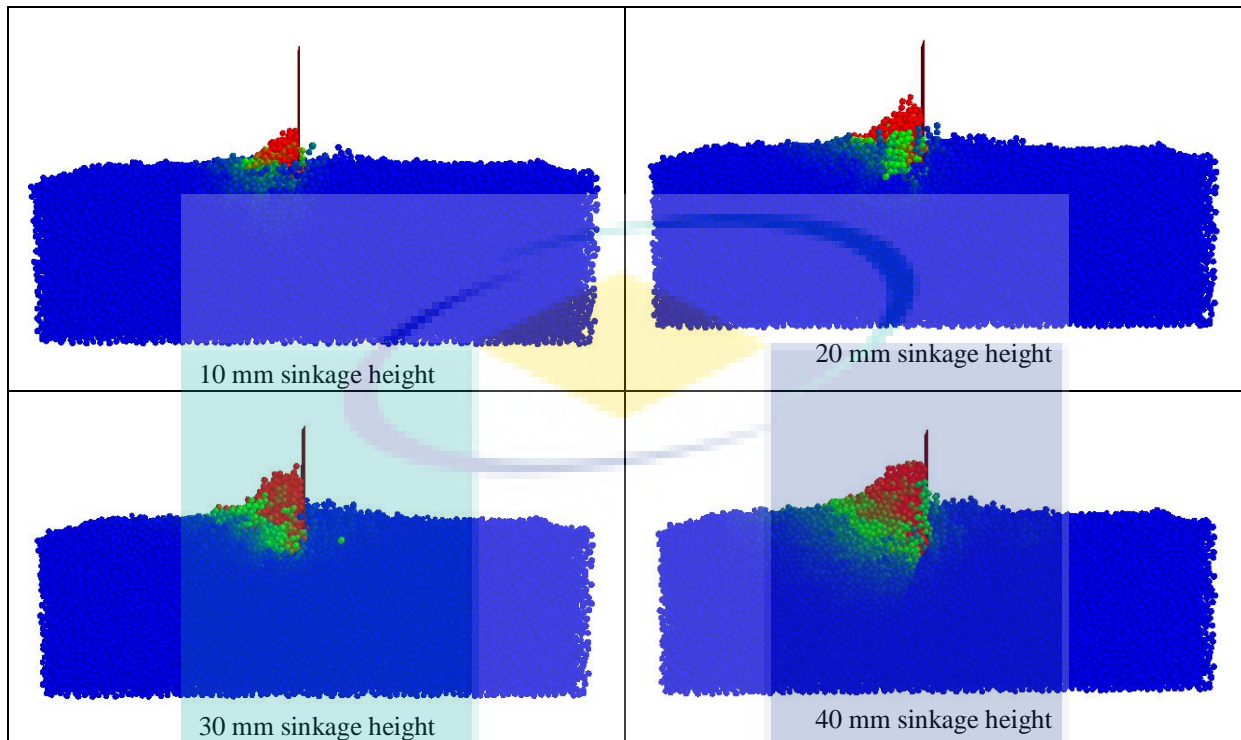
The generated normal force of the grouser surface may have related to the traction force of wheel. This assistive grouser model was designed to observe its efficiency before it was attached to a wheel. The relationship between normal force of the grouser and traction force of the wheel is where, when the normal force of the grouser is higher as the grouser moving (translational motion), it can be assume that when the grouser attach to the wheel, the traction force of the wheel will also higher and help the wheel to move forward. The forces generated when there is an interaction between the grouser surface and the sand particles. The higher the number of particles interact with the grouser surface, the higher the normal force (grouser surface) generated. The higher the normal force, the higher the traction force. And higher traction force help the wheel to move forward.

Based on the graph in Figure 5, grouser at sinkage height 40 mm generated higher normal force compared to the other sinkage height. So it can be assumed that the traction force at sinkage high 40 mm also higher compared to the other sinkage height. If the force generated is higher to the back of the wheel, it can help the wheel to move forward. But if the force generated is higher to the upward toward the surface, the wheel may have tendency to start digging into the sand. For this graph, the result is more focus on the force that generated with translation motion.

4.3.2 Grouser Translation Destructive Area

Destructive area is the area that was affected by the grouser movement. For this assistive grouser model, the grouser move with translation motion and the angle between the grouser and the sand surface is 90° (α). Every sinkage height shows different spread of destructive area. Table 4.2 below shows the images from simulation where the destructive area occurs for all sinkage height. The image was taken when the grouser stop moving.

Table 4.2: Destructive area from simulation model



From the images in Table 4.2, it can be observed that the higher the sinkage height, the bigger the destructive area affected. One of the reason is, when the sinkage height is higher, the contact between the surface and the sand particles is bigger. As the sinkage height higher, more number of particles interact with the grouser. This can be confirm by counting the number of particles that moves from the initial position of the grouser until its final position. At 10 mm sinkage height, the number of particles moved are 48524, while at 20 mm sinkage height 51830 particles moved, at 30 mm sinkage height 53875 particles moved and at 40 mm sinkage height 56390 particles moved. The amount of particles interact with the grouser generate the normal force of the grouser.

CHAPTER 5

CONCLUSION

5.1 Introduction

This chapter will conclude the finding in Chapter 4 as well as the next plan to continue this research study.

5.2 Simulation Conclusion for Conventional Rover and Modified Rover

In first set of simulation modelling, it was done to observe the relationship between particle movement and grouser motion direction by using DEM method for a wheel with a single grouser. The grouser used is fixed grouser for conventional wheel rover and assistive grouser for modified wheel rover. The result from the simulation of the particle-grouser interaction was recorded such as the distribution of velocity magnitude of each particles and the average sand displacement for each grouser angle range by each of rotation wheel.

From the velocity magnitude distribution, it can be observe that the affected particles for the fixed grouser were not limited to just the particles near the exact position of the grouser but extends to the particles at the back of the wheel. This mean if the wheel experiences high slippage for example on a steep slope, then the wheel will have a very high probability of digging and sinking into the sand as the sand is excavated from under the wheel towards the surface.

From average sand displacement result for 80 mm fixed grouser and 90 mm assistive grouser, it can be observe that 80 mm fixed grouser generated higher displacements in both X and Y direction. Although the longer grouser could generate higher forward traction, it also excavated more sand from under the wheel towards the surface causing the wheel to dig into the sand.

A longer fixed grouser could generate a large amount of traction due to the higher number of sand particles that interacts with the grouser, the rotating motion of a conventional fixed rover will also cause the longer grouser to displace a large amount of sand from under the wheel towards the back of the wheel increasing sinkage and also increase the wheel rotation resistance under high slippage conditions such as on a steep slope.

5.3 Assistive Grouser Model

This study was continue with assistive grouser model design. Assistive grouser was chosen instead of conventional grouser because from the previous simulation it is more suitable to be attached to the wheel. So this set of model is to observe which types of assistive grouser model is more suitable and give better efficiency when it attach with wheel rover. For this model, the assistive grouser was simulated at different sinkage height which is 10 mm, 20 mm, 30 mm and 40 mm. The main focus is to observed the normal force generated when the grouser interact with the sand particles at every sinkage height with translational motion. The sand surface is at level of inclination (0-degree inclination slope).

From the recorded result, it can be understand that sinkage height affect the normal force of grouser surface. The higher the sinkage height, the higher the normal force of the grouser surface. The normal force generated was affected by the number of particles interact with the grouser. The higher the sinkage height, the higher the number of particles interact with the grouser and the higher the normal force generated. Besides that, the different in sinkage height also affect the different in the destructive area after the grouser stop moving.

5.4 Future Work

This study will be continue by adjusting the sand surface inclination slope and the angle between the grouser and the sand surface (α). The different in surface inclination slope and α may have different result in force and destructive area.

References

1. *Rover - Exploring the Planets* [11/10/2017]; Available from: <https://airandspace.si.edu/exhibitions/exploring-the-planets/online/tools/rovers.cfm>.
2. Arvidson, R.E., et al., *Spirit Mars Rover Mission: Overview and selected results from the northern Home Plate Winter Haven to the side of Scamander crater*. J. Geophys. Res. , 2010. **115**.
3. Ibrahim, A.N., et al., *The Effect of Assistive Anchor-Like Grousers on Wheeled Rover Performance over Unconsolidated Sandy Dune Inclines*. Sensors (Basel), 2016. **16**(9).
4. Zhao, T., *Introduction to Discrete Element Method*, in *Coupled DEM-CFD Analyses of Landslide-Induced Debris Flows*. 2017. p. 25-45.
5. OSUMI, H., *Application of Robot Technologies to the Disaster Sites (Chapter 5)*. 2014, The Japan Society of Mechanical Engineers p. 58-73.
6. Nagatani., K., et al., *Emergency response to the nuclear accident at the Fukushima Daiichi Nuclear Power Plants using mobile rescue robots*. Journal of Field Robotics. **30**(1).
7. Nakashima, H., et al., *Discrete element method analysis of single wheel performance for a small lunar rover on sloped terrain*. Journal of Terramechanics, 2010. **47**(5): p. 307-321.

8. Sutoh., M., et al., *Traveling performance evaluation of planetary rovers on loose soil*. Journal of Field Robotics 2012. **29**(4): p. 648-662.
9. Smith, W.C., *Modeling of Wheel-Soil Interaction for Small Ground Vehicles Operating on Granular Soil* in *Mechanical Engineering* 2014, The University of Michigan
10. Smith, W., et al., *Comparison of DEM and Traditional Modeling Methods for Simulating Steady-State Wheel-Terrain Interaction for Small Vehicles* in *7th Americas Conference of the ISTVS* 2013: Tampa, Florida.
11. Wong., J., *Terramechanics and off-road vehicle engineering : terrain behaviour, off-road vehicle performance and design*. 2010, Amsterdam, The Netherlands: Butterworth-Heinemann.
12. Gertzos, K.P., P.G. Nikolakopoulos, and C.A. Papadopoulos, *CFD analysis of journal bearing hydrodynamic lubrication by Bingham lubricant*. Tribology International, 2008. **41**(12): p. 1190-1204.
13. Chen, P.Y.P. and E.J. Hahn, *Side clearance effects on squeeze film damper performance*. Tribology International, 2000(33): p. 161-165.
14. Ranjan, V., R. Pai, and D. Hargreaves, *Stiffness and damping coefficients of 3-axial grooved water lubricated bearing using perturbation technique*, in *In 5th EDF and LMS Poitiers Workshop 'Bearing Behaviour Under Unusual Operating Conditions', Futurescope*. 2006.
15. Gu, S., *Application of finite element method in mechanical design of automotive parts*, in *IOP Conference Series: Materials Science and Engineering*. 2017. p. 012180.
16. Silva, E.P.d., F.M.d. Silva, and R.R. Magalhães, *Application of Finite Elements Method for Structural Analysis in a Coffee Harvester*. Engineering, 2014. **06**(03): p. 138-147.
17. Cundall, P.A. and O.D.L. Strack, *Discrete numerical model for granular assemblies* Geotechnique, 1979. **29**(1): p. 47-65.
18. Nakashima, H. and T. Kobayashi, *Effects of gravity on rigid rover wheel sinkage and motion resistance assessed using two-dimensional discrete element method*. Journal of Terramechanics, 2014. **53**: p. 37-45.
19. Zhao, C.-L. and M.-Y. Zang, *Application of the FEM/DEM and alternately moving road method to the simulation of tire-sand interactions*. Journal of Terramechanics, 2017. **72**: p. 27-38.
20. Khot, L.R., et al., *Experiment validation of distinct element simulation for dynamic wheel-soil interaction*. Journal of Terramechanics, 2007: p. 429-437.
21. Sakaguchi, E., et al., *Simulation on discharging phenomena of grains by distinct element method - influence of shapes of element on flowing states*. J Jpn Soc Agr Machinery 1996. **54**(4): p. 9-17.
22. Feng, Y.T. and D.R.J. Owen, *An energy based corner to contact algorithm*. In: Cook BK, Jensen RP (Eds.), *Discrete element methods*, ACSE, 2002: p. 32-37.
23. Asaf, Z., I. Shmulevich, and D. Rubinstein, *Predicting soil-rigid wheel performance using distinct element methods*. Trans ASABE 2006. **49**(3): p. 607-16.
24. Wong, J.Y. and T. Kobayashi, *Further study of the method of approach to testing the performance of extraterrestrial rovers/rover wheels on earth*. Journal of Terramechanics, 2012.
25. Wong, J.Y., *Predicting the performances of rigid rover wheels on extraterrestrial surfaces based on test results obtained on earth*. Journal of Terramechanics, 2012. **49**(1): p. 49-61.
26. Nishiyama, K., et al., *2D FE-DEM analysis of tractive performance of an elastic wheel for planetary rovers*. Journal of Terramechanics, 2016. **64**: p. 23-35.
27. Patel, N., R. Slade, and J. Clemmet, *The ExoMars rover locomotion subsystem*. Journal of Terramechanics, 2010. **47**(4): p. 227-242.
28. Di, S., et al., *Effects of model size and particle size on the response of sea-ice samples created with a hexagonal-close-packing pattern in discrete-element method simulations*. Particulogy, 2017.

29. Zhang, H.P. and H.A. Makse, *Jamming transition in emulsions and granular materials*. Physical Review E, 2005. **72**(1): p. 011301.
30. Brilliantov, N.V., et al., *Model for collisions in granular gases*. Physical Review E, 1996. **53**(5): p. 5382-5392.
31. Silbert, L.E., et al., *Granular flow down an inclined plane: Bagnold scaling and rheology*. Physical Review E, 2001. **64**(5): p. 051302.
32. Johnson, K.L., K. Kendall, and A.D. Roberts. *Surface Energy and the Contact of Elastic Solids*. in *Proceedings of The Royal Society A: Mathematical, Physics and Engineering Science*. Sept 1971.
33. Smith, W. and H. Peng, *Modeling of wheel-soil interaction over rough terrain using the discrete element method*. Journal of Terramechanics, 2013. **50**(5): p. 277-287.
34. Plassiard, J.-P., N. Belheine, and F.-V. Donze, *A spherical discrete element model calibration procedure and incremental response*. Granular Matter 2009. **11**(5): p. 293-306.
35. Ibrahim, A.N.B., *Development of Assistive Anchor-Like Grousers for Improving Travel Performance of Wheeled Rover on Unconsolidated Sand Inclines*, in *School of Science and Engineering 2017*, Ibaraki University
36. Yang, Y., et al., *Characteristics of normal and tangential forces acting on a single lug during translational motion in sandy soil*. Journal of Terramechanics, 2014. **55**: p. 47-59.

